Roles of unsaturated fatty acids in autophagy.

A Doctoral Thesis

Submitted to Graduate School of Bioscience

Nagahama Institute of Bio-Science and Technology

Yuta Ogasawara

March 2015

Abstract of Dissertation

Autophagy is one of the major degradation pathways for cytoplasmic components. The autophagic isolation membrane is a unique membrane whose content of unsaturated fatty acids is very high. However, the molecular mechanisms underlying formation of this membrane, including the roles of unsaturated fatty acids, remain to be elucidated.

From a chemical library consisting of structurally diverse compounds, I screened for candidate inhibitors of starvation-induced autophagy by measuring LC3 puncta formation in mouse embryonic fibroblasts stably expressing GFP-LC3 (GFP-LC3 MEFs). As the results, I found several candidate inhibitors of autophagy. One of the candidate inhibitors, 2, 5-pyridinedicarboxamide, N2, N5-bis [5-[(dimethylamino)carbonyl]- 4-methyl-2-thiazolyl], has a molecular structure similar to that of a known stearoyl-CoA desaturase (SCD) 1 inhibitor.

To determine whether inhibition of SCD1 influences autophagy, I examined effects of the SCD1 inhibitor 28c on autophagy. This compound strongly inhibited starvation-induced autophagy, as determined by LC3 puncta formation, immunoblot analyses of LC3, electron-microscopic observations, and p62/SQSTM1 accumulation. Overexpression of SCD1 or supplementation with oleic acid which is a catalytic product of SCD1 abolished the inhibition of autophagy by 28c. Furthermore, 28c suppressed starvation-induced autophagy without affecting mTOR activity, and also inhibited rapamycin-induced autophagy.

In addition to inhibiting formation of LC3 puncta, 28c also inhibited formation of ULK1, WIPI1, Atg16L, and p62/SQSTM1 puncta during autophagy induction. These result suggested that SCD1 activity is required for the early stage of autophagy.

For further elucidating the role of SCD1, I used *Saccharomyces cerevisiae* as a model system. To examine the effect of deficiency of *OLE1* which is yeast homolog of SCD1, I constructed *ole1* mutants. The *ole1* mutants did not show nitrogen starvation-induced autophagy and intracellular transport by Cvt pathway in yeast, determined by ALP and Ape1 assay, respectively. These results clearly indicated that fatty acid desaturation is universally required for the autophagy in eukaryote cells.

Acknowledgements

First and foremost I would like to thank my parents, Miwako and Toshio Ogasawara for their encouragement throughout my life.

Next I would like to thank my thesis mentor, Processor Akitsugu Yamamoto for educating and helping me throughout this research.

I have been fortunate to have excellent collaborators within and outside of Nagahama Institute of Bio-Science and Technology. I would like to thank Professor Tamio Mizukami, Professor Noboru Mizushima and Professor Hiroyuki Arai and Dr. Atsuki Nara, Toru Komiya, Atsuko Iwamoto-Kihara for their guidance in my research. Special thanks go to Dr. Nozomu Kono for Fatty-acid analysis in Chapter III, and Dr. Yukio Mukai for his helpful discussions on the yeast genetic analysis of autophagy and the construction of *ole1* mutants in Chapter IV, and Dr. Eisuke Itakura for his helpful discussions on hierarchical analysis of autophagy.

Finally, I would like to thank my friends in the Yamamoto lab. and in Nagahama Institute of Bio-Science and Technology, for their encouragement: Mrs. Atsushi Nisizawa, Naoki Ozawa, Takuto Shigematsu, Shigeki Okamoto, Michiko Iwatsuki, Yuka Mori, Daiki Ishiyama, Takumi Kobayashi and Toshiyuki Kato.

Roles of unsaturated fatty acids in autophagy.
オートファジーにおける不飽和脂肪酸の役割

Table of contents

Chapter I

Introduction

Macroautophagy (hereafter referred to as autophagy) is a major pathway for degradation for cytoplasmic components. Autophagy plays roles in diverse physiological processes, including adaptation to starvation, clearance of intracellular proteins and damaged organelles, immunity, tumor suppression, and cell death (1). Autophagy is initiated by the emergence of an isolation membrane that encloses portions of the cytoplasm to form a double-membrane autophagosome. Autophagosomes fuse with endosomes and lysosomes sequentially to become autolysosomes, whose contents are degraded by lysosomal hydrolases. The isolation membrane is a unique membrane that contains several intramembrane particles (2, 3, 4) and a high content of unsaturated fatty acids (5). The origin of the isolation membrane has been the subject of a long-running debate (6).

Axe et al. (7) reported that isolation membranes arise from omegasomes, phosphatidylinositol 3-phosphate (PtdIns[3]P)–enriched domains of the ER. Hayashi-Nishino et al. showed that a subdomain of the ER forms a cradle encircling the isolation membrane, and that the ER membrane is interconnected to the isolation membrane (8). More recently, Hamasaki et al. (9) showed that autophagosomes form at ER–mitochondria contact sites. These observations strongly suggest the ER as a primary origin of the isolation membrane. However, the molecular mechanisms of autophagosome formation, including the dynamics of proteins and lipids and the role of the mitochondria, remain to be elucidated.

The discovery of autophagy-related genes (Atg) by Ohsumi and colleagues (10) tremendously accelerated studies of autophagy. The kinase Atg1 (ULK1 in mammals), which forms a complex with Atg13/Atg101/FIP200 (11, 12), is an upstream regulator of the Atg protein cascades. Under nutrient-rich condition, the serine-threonine kinase mTOR phosphorylates and suppresses ULK1. After starvation, mTOR activity is depressed, and ULK1 is dephosphorylated, resulting in its activation (13). AMP-dependent kinase (AMPK) also activates ULK1 by phosphorylating different sites from those targeted by mTOR (14). Activated ULK1/Atg13/Atg101/FIP200 complex is recruited to sites of autophagosome formation, which correspond to omegasomes. The localization pattern of the complex changes from diffuse to punctate during the formation of autophagosomes. Simultaneously, the PtdIns3-kinase complex Vps34/Vps15/Beclin-1 is recruited to autophagosome formation sites on the ER via Atg14L. This complex is activated by phosphorylation of Beclin-1 by ULK1 (15); when activated, the complex produces PtdIns(3)P (16). Subsequently,

PtdIns(3)P-binding proteins such as WIPI1 (17) and DFCP1 (7), the Atg12/Atg5/Atg16L complex (18), and LC3 (19) are also recruited to sites of autophagosome formation, and these proteins form puncta in a hierarchical manner (20). However, the details of the underlying biochemical cascades remain obscure.

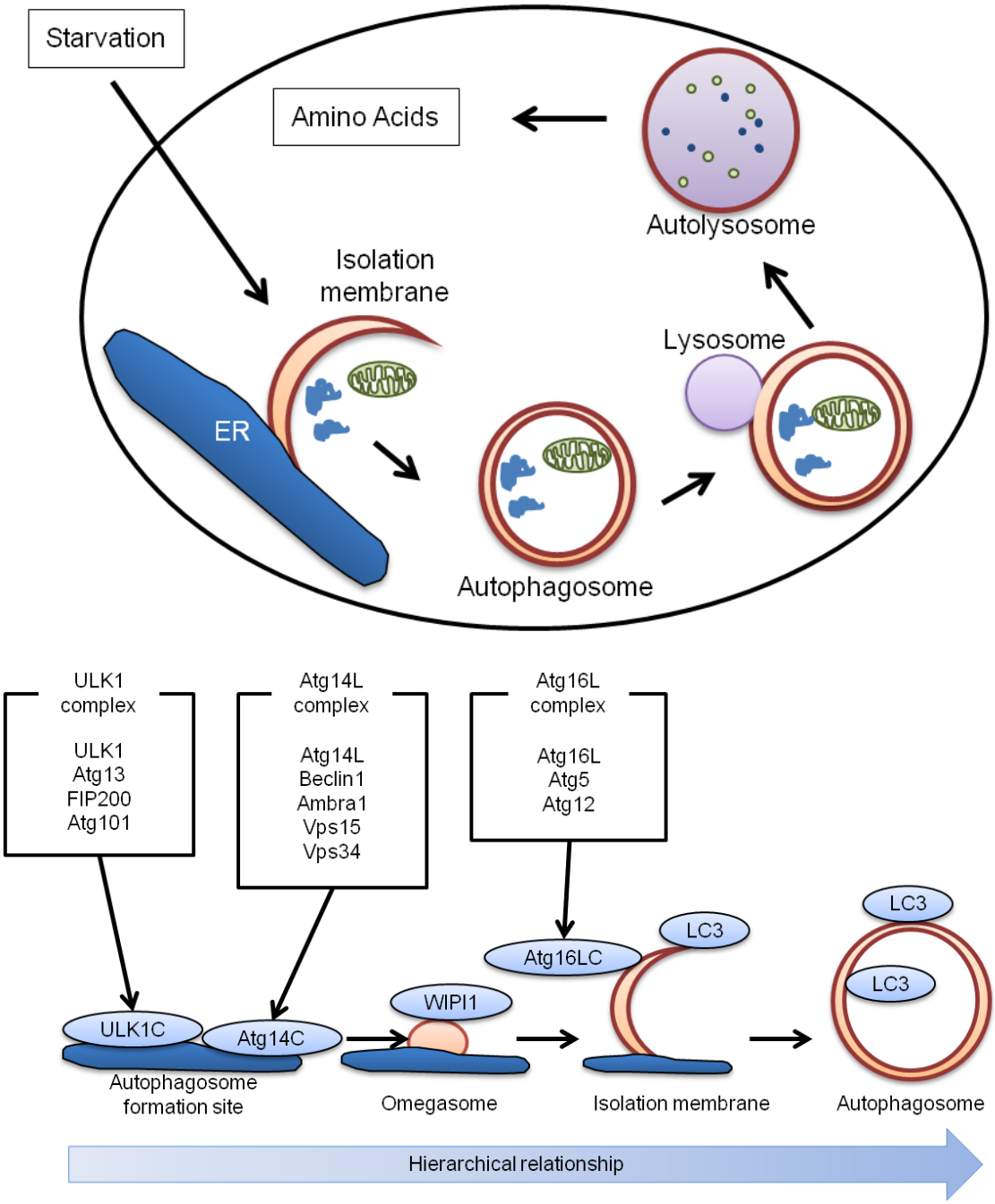

Figure 1. Schematic and molecular mechanism of autophagy.

References

1. Mizushima, N., Levine, B., Cuervo, A. M., Klionsky, D. J. (2008) Autophagy fights disease through cellular self-digestion. Nature. 451, 1069-1075
2. Hirsimäki, Y., Hirsimäki, P., Lounatmaa, K. (1982) Vinblastine-induced autophagic vacuoles in mouse liver and Ehrlich ascites tumor cells as assessed by freeze-fracture electron microscopy. Eur J Cell Biol. 27, 298-301
3. Fengsrud, M., Erichsen, E. S., Berg, T. O., Raiborg, C., Seglen, P. O. (2000) Ultrastructural characterization of the delimiting membranes of isolated autophagosomes and amphisomes by freeze-fracture electron microscopy. Eur J Cell Biol. 79, 871-882
4. Réz, G., Meldolesi, J. (1980) Freeze-fracture of drug-induced autophagocytosis in the mouse exocrine pancreas. Lab Invest. 43, 269-277
5. Reunanen, H., Punnonen, E. L., Hirsimäki, P. (1985) Studies on vinblastine-induced autophagocytosis in mouse liver. V. A cytochemical study on the origin of membranes. Histochemistry. 83, 513-517
6. Juhasz, G., Neufeld, T. P. (2006) Autophagy: a forty-year search for a missing membrane source. PLoS Biol. 4, e36
7. Axe, E. L., Walker, S. A., Manifava, M., Chandra, P., Roderick, H. L., Habermann, A., Griffiths, G., Ktistakis, N. T. (2008) Autophagosome formation from membrane compartments enriched in phosphatidylinositol 3-phosphate and dynamically connected to the endoplasmic reticulum. J Cell Biol. 182, 685-701
8. Hayashi-Nishino, M., Fujita, N., Noda, T., Yamaguchi, A., Yoshimori, T., Yamamoto, A. (2009) A subdomain of the endoplasmic reticulum forms a cradle for autophagosome formation. Nat Cell Biol. 11, 1433-1437
9. Hamasaki, M., Furuta, N., Matsuda, A., Nezu, A., Yamamoto, A., Fujita, N., Oomori, H., Noda, T., Haraguchi, T., Hiraoka, Y., Amano, A., Yoshimori, T. (2013) Autophagosomes form at ER-mitochondria contact sites. Nature. 495, 389-393
10. Ohsumi, Y. (1999) Molecular mechanism of autophagy in yeast, Saccharomyces cerevisiae. Philos Trans R Soc Lond B Biol Sci. 354, 1577-1581
11. Hara, T., Takamura, A., Kishi C., Iemura, S., Natsume, T., Guan, J. L., Mizushima, N. (2008) FIP200, a ULK-interacting protein, is required for autophagosome formation in mammalian cells. J Cell Biol. 181, 497-510.
12. Mercer, C. A., Kaliappan, A., Dennis, P. B. (2009) A novel, human Atg13 binding protein, Atg101, interacts with ULK1 and is essential for macroautophagy. Autophagy. 5, 649-662.
13. Hosokawa, N., Hara, T., Kaizuka, T., Kishi, C., Takamura, A., Miura, Y., Iemura, S.,

Natsume, T., Takehana, K., Yamada, N., Guan, J. L., Oshiro, N., Mizushima, N. (2009) Nutrient-dependent mTORC1 association with the ULK1-Atg13-FIP200 complex required for autophagy. Mol Biol Cell. 20, 1981-1991

14. Kim, J., Kundu, M., Viollet, B., Guan, K. L. (2011) AMPK and mTor regulate autophagy through direct phosphorylation of Ulk1. Nat Cell Biol. 13, 132-141
15. Russell, R. C, Tian, Y., Yuan, H., Park, H.W., Chang, Y.Y., Kim, J., Kim, H., Neufeld, T. P., Dillin, A., Guan, K. L. (2013) ULK1 induces autophagy by phosphorylating Beclin-1 and activating VPS34 lipid kinase. Nat Cell Biol. 15, 741-750.
16. Matsunaga, K., Morita, E., Saitoh, T., Akira, S., Ktistakis, N. T., Izumi, T., Noda, T., Yoshimori, T. (2010) Autophagy requires endoplasmic reticulum targeting of the PI3-kinase complex via Atg14L. J Cell Biol. 190, 511-521.
17. Proikas-Cezanne, T., Waddell, S., Gaugel, A., Frickey, T., Lupas, A., Nordheim, A. (2004) WIPI-1alpha (WIPI49), a member of the novel 7-bladed WIPI protein family, is aberrantly expressed in human cancer and is linked to starvation-induced autophagy. Oncogene. 23, 9314-9325
18. Fujita, N., Itoh, T., Omori, H., Fukuda, M., Noda, T., Yoshimori, T. (2008) The Atg16L complex specifies the site of LC3 lipidation for membrane biogenesis in autophagy. Mol Biol Cell. 19, 2092-2100
19. Kabeya, Y., Mizushima, N., Ueno, T., Yamamoto, A., Kirisako, T., Noda, T., Kominami, E., Ohsumi, Y., Yoshimori, T. (2000) LC3, a mammalian homologue of yeast Apg8p, is localized in autophagosome membranes after processing. EMBO J. 19, 5720-5728
20. Itakura, E., Mizushima, N. (2010) Characterization of autophagosome formation site by a hierarchical analysis of mammalian Atg proteins. Autophagy. 6, 764-776

Chapter II. Screening of inhibitors of autophagy

Abstract

Autophagy is one of the major degradation pathways for cytoplasmic components. The autophagic isolation membrane is a unique membrane whose content of unsaturated fatty acids is very high. However, the molecular mechanisms underlying formation of this membrane, including the roles of unsaturated fatty acids, remain to be elucidated. To elucidate the molecular mechanism of autophagy, I tried screening of inhibitors of autophagy from the small-molecule library consisting of 528 synthetic compounds which are designed with an emphasis on structural diversity. In this screen, I identified several candidate inhibitors of autophagy determined by counting of GFP-LC3 puncta which correspond to the autophagosomes in mouse embryonic fibroblasts stably expressing GFP-LC3 (GFP-LC3 MEFs) using fluorescence microscope. Furthermore, I found that one of the candidate inhibitors, No. 73 inhibit starvation induced autophagy and is structurally similar to stearoyl-CoA desaturase (SCD) 1 inhibitor.

Introduction

The discovery of drugs that target autophagy, such as 3-methyladenine and rapamycin, has contributed greatly to elucidation of the mechanisms of autophagy (21 , 22). To date, many autophagy-inducing agents (e.g., rapamycin) have been discovered, but only a small number of inhibitors of autophagy have been reported. Two well-known inhibitors of autophagy are 3-methyladenine and wortmannin, both of which suppress autophagosome formation at the same step, production of PtdIns(3)P, by inhibiting PtdIns3-kinase (23). Identification of new inhibitors of autophagy will be essential in order to advance the study of autophagy.

In this study, I identified several candidate inhibitors of autophagy by screening a chemical library consisting of structurally diverse small molecules. In this screen, I counted GFP-LC3 puncta which correspond to the autophagosomes after starvation in mouse embryonic fibroblasts stably expressing GFP-LC3 (GFP-LC3 MEFs). Of the candidate inhibitors, NO. 73: 2,5-pyridinedicarboxamide, N2, N5-bis[5-[(dimethylamino)carbonyl]-4-methyl-2-thiazolyl] inhibited not only puncta formation of GFP-LC3 but also conversion LC3-I to LC3-II after starvation. These result suggested that No. 73 inhibited starvation induced autophagy. I also found that No. 73 is structurally similar to a previously known stearoyl-CoA desaturase (SCD) 1 inhibitor (24).

Experimental procedures

Small-molecule screening library–An in-house small-molecule library consisting of 528 synthetic compounds was designed with an emphasis on structural diversity (unpublished), and used to screen for novel inhibitors of autophagy. These chemicals were dissolved in DMSO at a concentration of 2 mg/ml, stored as stock solutions at -30°C, and used at final concentrations of 10–20 μg/ml for screening.

Cell culture and treatment with chemicals–GFP-LC3 MEFs were cultured in regular medium: Dulbecco's modified Eagle medium (DMEM) with 10% fetal bovine serum (FBS) and 2 mM L-glutamine (L-Gln) under 5% CO2. To induce autophagy, cells were incubated for 2 hours in starvation medium (Earle's balanced salt solution, EBSS). For chemical treatment, cells were incubated for 2 hours in starvation medium containing 10 μ g/ml of the chemicals.

Measurement of autophagy by fluorescent microscopy–Cells expressing GFP-LC3 in culture medium were washed with phosphate-buffered saline (PBS) and fixed in 4% paraformaldehyde in 0.1 M phosphate buffer, pH 7.4 (PB), for 10 min. Cells were washed in PBS three times for 5 min, and then observed under an Axiovert 200 fluorescence microscope (Zeiss, Gottingen, Germany). For quantitative analyses, micrographs were taken randomly, and the numbers of GFP-LC3 puncta per cell were counted. It is regarded the chemicals that reduced number of GFP-LC3 puncta to less than 30, as candidate inhibitors.

Chemical information–Information regarding structurally similar compounds was obtained from SciFinder.

Immuno-blot analysis–Cells were lysed in SDS sample buffer: 0.05 M Tris-HCl (pH 6.8), 2% SDS, 6% β-mercaptoethanol, 10% glycerol, and 1% BPB. Protein contents of cell lysates were determined by RCDC assay (Bio-Rad, Hercules, California), and equal amounts of protein (30 μg) were electrophoresed through 12% polyacrylamide gels and transferred to polyvinylidene difluoride (PVDF) membranes (GE Healthcare, Little Chalfont, UK). Membranes were blocked with 5% non-fat milk and subsequently incubated for 1 hour with rabbit anti-LC3 antibody obtained from Novus Biologicals (Littleton, CO, USA) or mouse anti-α-tubulin antibody obtained from Sigma-Aldrich (St. Louis, MO, USA), and then incubated with Horseradish peroxidase (HRP)-conjugated goat anti–rabbit IgG or anti–mouse IgG antibodies obtained from Jackson ImmunoResearch Laboratories (West Grove, PA, USA), followed by exposure to ECL detection reagents (GE Healthcare). Densitometric analysis was performed using electrophoresis analysis software (Fujifilm Co., Tokyo, Japan).

Results

In order to identify candidate inhibitors of autophagy, I screened a chemical library consisting of 528 structurally diverse compounds by monitoring the effect of each compound on formation of GFP-LC3 puncta in GFP-LC3 MEFs. LC3 is synthesized as precursor which is immediately cleaved the C-terminal peptide by Atg4. Cleaved form of LC3, called LC3-I which localized in cytoplasm binds to phosphatidylethanolamine (PE) trough C-terminas glycine after starvation. PE conjugated LC3, called LC3-II binds to autophagosome membranes, therefore LC3 is used as marker protein of autophagy. Inhibition of GFP-LC3 puncta formation was the principal criterion for identification of inhibitors of autophagy.

In regular medium, GFP-LC3 MEFs exhibited diffuse fluorescence throughout the cytoplasm, whereas many fluorescent puncta corresponding to autophagosomes appeared after cells were transferred to starvation medium for 2 hours (Fig. 2A). As a result of the screening, I found that No. 33, No.61, No.73 or No. 382 inhibit GFP-LC3 puncta formation after starvation (Fig. 2B and C). I also demonstrated that the one of the candidate inhibitors, No. 73, 2,5-pyridinedicarboxamide, N2, N5-bis[5-[(dimethylamino)carbonyl]-4-methyl-2- thiazolyl], strongly suppressed starvation-induced autophagy in GFP-LC3 MEFs after 2 h at a concentration of 20 μg/ml (Fig. 2D and E). The concentration of No. 73 that decreased the number of GFP-LC3 puncta by 50% (IC50) was ~2.5 μg/ml (~7 μM) in GFP-LC3 MEFs (Fig. 2D).

Immunoblot analysis were also used to demonstrate induction of autophagy, in particular by monitoring the processing of the LC3-I, cytoplasmic form into the LC3-II, autophagosome bound form. These two types of LC3 can be distinguished on immunoblots, because the apparent molecular weight of LC3-II is lower than that of LC3-I. When NIH3T3 cells were transferred to starvation medium from regular medium, the content of LC3-II increased, whereas this increase in LC3-II level was strongly suppressed when cells were transferred into starvation medium containing No. 73 (Fig. 2E).

Because bioactivity of No. 73 was unknown, I performed similarity search based on the structure using SciFinder which is a Chemical database. I found that No. 73 is structurally similar to a previously known SCD1 inhibitor (24) by the similarity search.

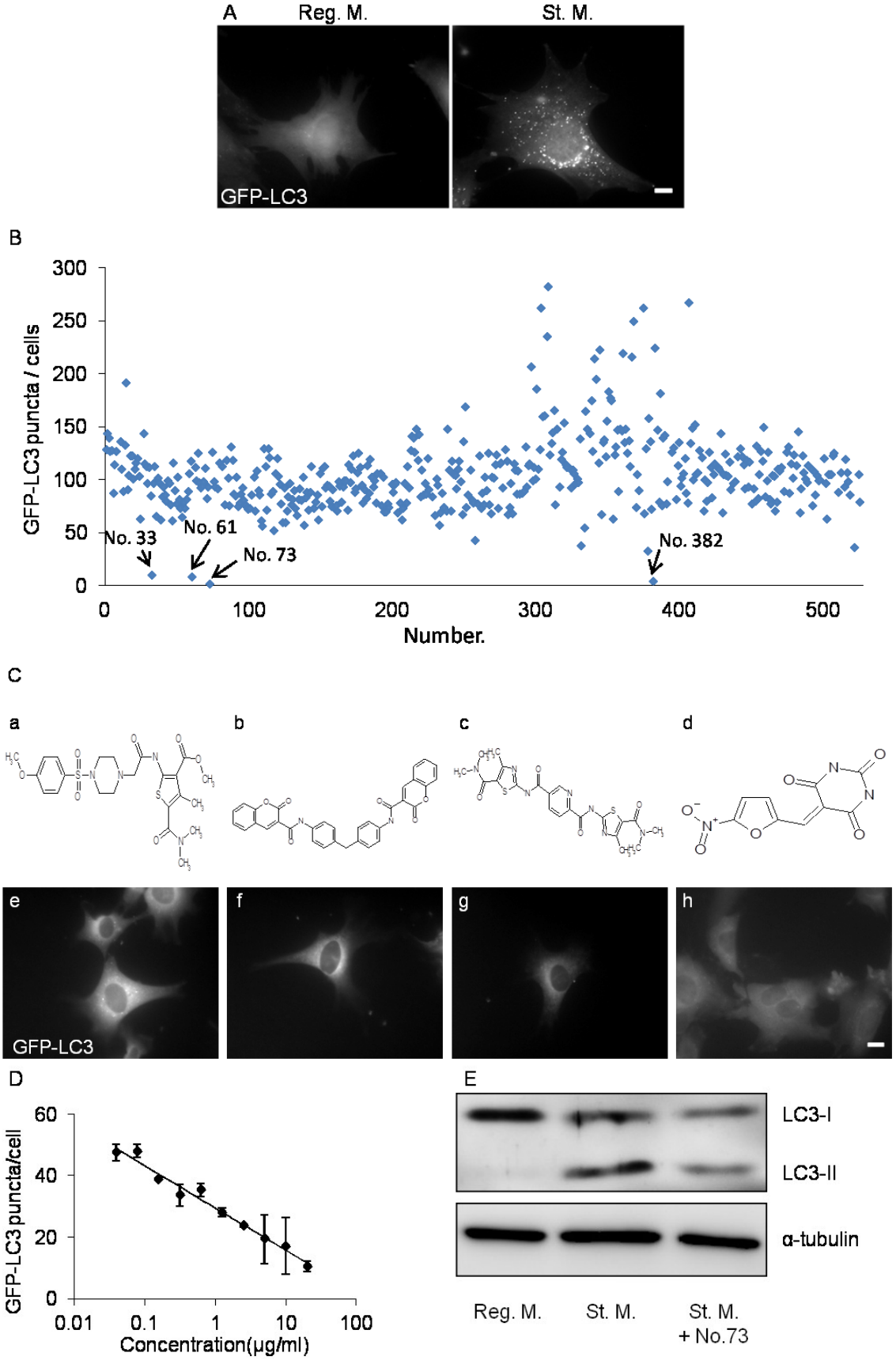
A
Reg. M.
St. M.
GFP-LC3
B
GFP-LC3 puncta / cells
300
250
200
150
100
50
0
No. 33
No. 61
No. 73
No. 382
0
100
200
300
400
500
Number.
C
a
b
c
d
e
f
g
h
GFP-LC3
D
GFP-LC3 puncta/cell
60
40
20
0
0.01
0.1
1
10
100
Concentration(μg/ml)
E
LC3-I
LC3-II
α-tubulin
Reg. M.
St. M.
St. M.
+ No.73

Figure 2. No. 33, No.61, No.73 or No. 382 inhibited starvation induced puncta formation of GFP-LC3. (A) GFP-LC3 MEFs were cultured for 2 h in regular medium (Reg. M.) or starvation medium (St. M.). (B) Screening of inhibitors of autophagy. GFP-LC3 MEFs were cultured for 2 h in starvation medium with 10 μg/ml of the indicated chemical compound. Numbers of GFP-LC3 puncta per cell were counted. Data represent means of 5 cells. (C) Chemical structures of No. 33 (a), No. 61 (b), No. 73 (c) and No.382 (d). GFP-LC3 MEFs were cultured for 2 h in starvation medium with 10 μg/ml of No. 33 (e), No. 61 (f), No. 73 (g) and No.382 (h). Scale bars, 10 μm. (D) Dose-dependent inhibition of formation of GFP-LC3 puncta by No. 73. Numbers of GFP-LC3 puncta per cell were counted. Data represent means ± SE of three independent experiments, in each of which more than 30 cells were counted. (E) NIH3T3 cells were cultured for 2 h in regular medium, starvation medium, or starvation medium with 20 μg/ml No. 73. Cell lysates were processed for immunoblot analysis to detect LC3 and α-tubulin (as an endogenous control).

Discussion

In this study, I screened inhibitors of autophagy from a chemical library consisting of structurally diverse small molecules. As a result, I identified No. 33, No. 61, No. 73 and No. 382 as candidate inhibitors determined by counting of GFP-LC3 puncta in GFP-LC3 MEFs after starvation. Furthermore, No. 73 dose-dependently inhibited puncta formation of GFP-LC3, and suppressed conversion LC3-I to LC3-II suggesting that starvation induced autophagy is suppressed. I also found that No. 73 is structurally similar to a SCD1 inhibitor. Although participation of SCD1 in mammalian autophagy is unknown, Köhler et al. reported that that autophagy is suppressed by knockout of a *Drosophila* SCD homolog, Desat1 (25). Next, I investigated whether a SCD1 inhibitor suppressed starvation induced autophagy.

Reference

21. Seglen, P. O., Gordon, P. B. (1982) 3-Methyladenine: specific inhibitor of autophagic/lysosomal protein degradation in isolated rat hepatocytes. Proc Natl Acad Sci U S A. 79, 1889-1892
22. No.da, T., and Ohsumi, Y. (1998) Tor, a Phosphatidylinositol Kinase Homologue, Controls Autophagy in Yeast . J. Biol. Chem. 273, 3963-3966.
23. Miller, S., Tavshanjian, B., Oleksy, A., Perisic, O., Houseman, B. T., Shokat, K. M., Williams, R. L. (2010) Shaping development of autophagy inhibitors with the structure of the lipid kinase Vps34. Science. 327, 1638-1642

24. Iida, T., Mitani, I., Nakagawa, Y., Tanaka, M., (2008) Preparation of six-membered heterocyclic amide and benzamide derivatives as stearoyl-CoA desaturase 1 (SCD1) inhibitors. PCT Int. Appl.
25. Köhler, K., Brunner, E., Guan, X. L., Boucke, K., Greber, U. F., Mohanty, S., Barth, J. M., Wenk, M. R., Hafen, E. (2009) A combined proteomic and genetic analysis identifies a role for the lipid desaturase Desat1 in starvation-induced autophagy in Drosophila. Autophagy. 5, 980-990

Chapter III. Analysis of role of SCD1 activity in mammalian autophagic process.

Abstract

The limiting membrane of autophagosomes is thought to be a unique membrane whose content of unsaturated fatty acids is very high. However, the molecular mechanisms of the formation of the membrane, including the dynamics of proteins and lipids remain to be elucidated. In the screening of inhibitor of autophagy, I found that No. 73 inhibits starvation induced autophagy and is structurally similar to a SCD 1 inhibitor. This result suggested that SCD1 activity is required for autophagy.

To determine whether SCD1 inhibition influences autophagy, I examined the effects of the SCD1 inhibitor 28c. This compound strongly inhibited starvation-induced autophagy, as determined by LC3 puncta formation, immunoblot analyses of LC3, electron-microscopic observations, and p62/SQSTM1 accumulation. Overexpression of SCD1 or supplementation with oleic acid which is a catalytic product of SCD1 abolished the inhibition of autophagy by 28c. Furthermore, 28c suppressed starvation-induced autophagy without affecting mTOR activity, and also inhibited rapamycin-induced autophagy. In addition to inhibiting formation of LC3 puncta, 28c also inhibited formation of ULK1, WIPI1, Atg16L, and p62/SQSTM1 puncta. These results suggest that SCD1 activity is required for the earliest step of autophagosome formation.

Introduction

Novel autophagy inhibitor No. 73 is structurally similar to a SCD1 inhibitor (24). However, participation of SCD1 in mammalian autophagy was unknown. SCD1 is an integral membrane protein of the ER, and a key enzyme for the biosynthesis of mono-unsaturated fatty acids (MUFA) from saturated fatty acids (SFA). The principal product of SCD1 is oleic acid, which is formed by desaturation of stearic acid. Products of SCD1 serve as substrates for the synthesis of various kinds of lipids, including phospholipids, triglycerides, cholesteryl esters, wax esters, and alkyldiacylglycerols. The genes encoding SCD have been cloned from various species, including yeast, Drosophila, C. elegans, sheep, hamster, rat, mouse, and human. In mouse, four isoforms (SCD-1, SCD-2, SCD-3, and SCD-4) have been identified, whereas in human, there are two (SCD1 and SCD5) (26).

In this study, I investigated role of SCD1 in mammalian autophagy using SCD1 inhibitor 28c (27). I demonstrated that 28c suppresses starvation induced autophagy. During my study of the role of SCD1 in mammalian autophagy, I became aware of a report from Köhler et al. demonstrating that autophagy is suppressed by knockout of a

Drosophila SCD1 homolog, Desat1 (25). Although that study did not reveal the processes of autophagy that require SCD1 in Drosophila, those results, in conjunction with the results of my study, suggest that SCD activity may be generally important for autophagy. Mine is the first report that demonstrates a requirement for SCD1 activity in mammalian autophagy.

Experimental procedures

Chemicals–Rapamycin and bafilomycin A_1 were purchased from Wako Pure Chemical Industries. Ltd. (Osaka, Japan); dissolved in DMSO at concentrations of 5 mM and 100 μM, respectively; stored as stock solutions at -30°C; and used at final concentrations of 1 μM and 100 nM, respectively. The SCD1 inhibitor 28c was purchased from Santa Cruz Biotechnology, Inc. (sc205109, Dallas, TX, USA), diluted in DMSO as a stock solution (10 mg/ml), stored at -30°C, and used within a few months at a final concentration of 20 μg/ml. SCD1 siRNAs were used at a final concentration of 10 nM. Oleic acid–BSA conjugates (OA-BSA) were purchased from Sigma-Aldrich (St. Louis, MO, USA), and used at a final concentration of 500 μM. Palmitic acid–BSA conjugates (PA-BSA) were prepared by a modification of the method of Hannah et al. (28). Palmitic acid (PA) was purchased from Cayman Chemical (Ann Arbor, MI, USA). PA was dissolved in ethanol at 100 mM, and this stock solution was stored at 4°C. PA solution (50 μl) was precipitated with 62.5 μl of 2 N NaOH, and 387.5 μl of ethanol was added. The resultant solution was evaporated under nitrogen gas, and then reconstituted with 1 ml of pre-warmed saline. Then, 1.25 ml of 10% BSA (fatty acid free, Sigma-Aldrich, St. Louis, MO, USA) dissolved in saline was added to this solution; the pH was adjusted to 7.0 with 2 N HCl; and saline was added to a volume of 2.5 ml. The resultant solution was filtered and stored at -30°C.

Antibodies–Rabbit anti-GFP antibody was kindly provided by Professor Nobuhiro Nakamura (Kyoto Sangyo University, Japan). Rabbit anti-LC3 antibody was obtained from Novus Biologicals (Littleton, CO, USA). Mouse anti-LC3 antibody and rabbit anti-Atg16L antibody were from Cosmo Bio Co., Ltd. (Tokyo, Japan). Guinea pig polyclonal anti-p62/SQSTM1 antibody was from Progen Biotechnik GmbH (Heidelberg, Germany). Hamster monoclonal anti-Atg9A antibody was from Abcam (Cambridge, UK). Rabbit anti–phospho-AMPKα (Thr 172) antibody, rabbit anti–S6 ribosomal protein antibody, and rabbit anti–phospho-S6 ribosomal protein (Ser 235/236) antibody were from Cell Signaling Technology, Inc. (Danvers, MA, USA). Rabbit anti-SCD1 antibody was from Santa Cruz Biotechnology. Mouse anti-α-tubulin antibody was from Sigma-Aldrich. Goat anti-rabbit IgG, anti-hamster IgG and

anti-guinea pig antibody conjugated to Alexa Fluor 546 were from Invitrogen (Carlsbad, CA, USA). Horseradish peroxidase (HRP)-conjugated goat anti–rabbit IgG, anti–mouse IgG, and anti–guinea pig IgG antibodies were from Jackson ImmunoResearch Laboratories (West Grove, PA, USA).

Cell culture and treatment with chemicals–In this study, I used MEFs stably expressing GFP-LC3, GFP-ULK1 (20), or GFP-WIPI1 (20) mainly for analysis of puncta formation; MEFs stably expressing GFP-p62/SQSTM1 (GFP-p62/SQSTM1 MEFs) (29) for immunoblot analysis of p62/SQSTM1; NIH3T3 cells for immunoblot and SCD1-overexpression experiments; and HeLa cells for knockdown experiments and immunofluorescence microscopy. GFP-LC3 MEFs were kindly provided by Professor Tamotsu Yoshimori (Osaka University, Japan). GFP-LC3 MEFs, GFP-p62/SQSTM1 MEFs, HeLa cells and NIH3T3 cells were cultured in regular medium: Dulbecco's modified Eagle medium (DMEM) with 10% fetal bovine serum (FBS) and 2 mM L-glutamine (L-Gln) under 5% CO2. MEFs stably expressing WIPI1 and ULK1 were maintained in DMEM containing 10% FBS, 2 mM L-Gln, and 1 μg/ml puromycin (20). To induce autophagy, cells were incubated for 2 hours in starvation medium (Earle's balanced salt solution, EBSS). For chemical treatment, cells were incubated for 2 hours in starvation medium containing the indicated chemicals. For addition of oleic acid (OA) or palmitic acid (PA), cells were incubated in regular or starvation medium containing 500 μM OA-BSA conjugate or 100 μM PA-BSA conjugate. As vehicle control, 1.25% BSA was used.

Knock down of SCD1–RNA interference against SCD1 was carried out as described in Ariyama et al. (30). In brief, HeLa cells were transfected with SCD1 siRNAs at a final concentration of 10 nM using Lipofectamine RNAiMAX (Invitrogen). Cells were then cultured in regular medium for 72 hours.

Immuno-blot analysis–Cells were lysed in SDS sample buffer: 0.05 M Tris-HCl (pH 6.8), 2% SDS, 6% β-mercaptoethanol, 10% glycerol, and 1% BPB. Protein contents of cell lysates were determined by RCDC assay (Bio-Rad, Hercules, California), and equal amounts of protein (30 μg) were electrophoresed through 12% polyacrylamide gels and transferred to polyvinylidene difluoride (PVDF) membranes (GE Healthcare, Little Chalfont, UK). Membranes were blocked with 5% non-fat milk and subsequently incubated for 1 hour with rabbit anti-LC3 antibody, guinea pig anti-p62/SQSTM1 antibody, rabbit anti-SCD1 antibody, or mouse anti-α-tubulin antibody, and then incubated with HRP-conjugated anti-rabbit, anti–guinea pig, or anti-mouse IgG antibody followed by exposure to ECL detection reagents (GE Healthcare). Densitometric analysis was performed using electrophoresis analysis software (Fujifilm

Co., Tokyo, Japan).

Measurement of autophagy by fluorescent microscopy–Cells expressing GFP-LC3 in culture medium were washed with phosphate-buffered saline (PBS) and fixed in 4% paraformaldehyde in 0.1 M phosphate buffer, pH 7.4 (PB), for 10 min. Cells were washed in PBS three times for 5 min, and then observed under an Axiovert 200 fluorescence microscope (Zeiss, Gottingen, Germany). For quantitative analyses, micrographs were taken randomly, and the numbers of LC3 puncta per cell were counted.

Immunofluorescence Microscopy–MEFs in culture medium were washed with PBS and fixed in 4% paraformaldehyde in PB for 10 min. After fixation, the cells were permeabilized with 100 μg/ml digitonin or 0.01% Triton X-100 in PBS for 10 min, and then blocked for 30 min with blocking solution (PBS containing 2% BSA and 2% goat serum). The cells were then incubated for 30 min with rabbit anti-Atg16L serum (diluted 200×), mouse anti-LC3 antibody (1 μg/ml), or hamster monoclonal anti-Atg9A antibody (10 μg/ml) diluted in blocking solution. After washing, cells were incubated for 30 min with the appropriate secondary antibodies (goat anti-rabbit IgG, goat anti-mouse IgG or goat anti-hamster IgG conjugated with Alexa Fluor 546) diluted in blocking solution, and then washed with PBS. Finally, the cells were observed under an Axiovert 200 fluorescence microscope. For confocal microscopy, a Fluoview FV1000 (Olympus, Tokyo, Japan) was used.

Electron microscopy–Cells were cultured on Cell Desk substrates (Sumitomo Bakelite Co., Ltd, Tokyo, Japan) in 24-well plates. Cells were fixed in 2% glutaraldehyde in PB for 1 hour. The cells were washed in PBS three times, and post-fixed for 1 hour in PB containing 1% OsO4 (TAAB, Berks, UK) and 1.5% potassium ferrocyanide. After being washed in distilled water, cells were dehydrated with a graded series of ethanol and embedded in epoxy resin (TAAB). Ultrathin sections were doubly stained with uranyl acetate and lead citrate, and observed under an H7600 electron microscope (Hitachi, Tokyo, Japan). For quantitative analyses, electron micrographs were taken randomly using a H7600 electron microscope equipped with ORIUS™ SC200W 2k × 2 k TEM CCD camera (Gatan Inc. CA) at a magnification of 8,000×. The surface areas of autophagosomes and autolysosomes were measured using the MacSCOPE 2.5 software (Mitani Corporation, Fukui, Japan). Surface areas of autophagosomes and autolysosomes were normalized to the cytoplasmic area.

Quantitative RT-PCR–Total RNA from NIH3T3 cells was prepared using ISOGEN (Nippon Gene, Tokyo, Japan). Quantitative real-time RT-PCR was performed using the QuantiTect SYBR® Green RT-PCR Kit (Qiagen, CA, USA). All data were

normalized to the level of β-actin (*Actb*) expression in the same sample. The following primers were used: p62/SQSTM1, p62/Sqstm1-5' (5'-GCCAGAGGAACAGATGGAGT-3') and p62/Sqstm1-3' (5'-TCCGATTCTGGCATCTGTAG -3'); β-actin, Actb-5' (5'-TCCCTGGAGAAGAGCTACGA-3') and Actb-3' (5'-AGCACTGTGTTGGCGTACAG-3').

Cloning of SCD1 and plasmid transfection– Total RNA from NIH3T3 cells was prepared using ISOGEN. Synthesis of first-strand cDNA was performed using the StrataScript First-Strand Synthesis System (Stratagene, La Jolla, CA). The cDNA encoding mouse SCD1 was then amplified by PCR using primers mSCD1-5 (5'-ATAACCGAATTCATGCC GGCCCACATGCT) and mSCD1-3 (5'- GCTCA ACTGCAGTCAGCTACTCTTGTGACTCC). This SCD1 cDNA was subcloned into the *Eco*RI-*Pst*I sites of pEGFP-C2 (Clontech Laboratories, Inc., Palo Alto, CA), and the resultant plasmid was used for expression of the GFP fusion protein. The construct was verified by DNA sequencing. For transfection, I used the HilyMax system (Dojindo Molecular Technologies, Inc., Gaithersburg, MD, USA). Cells were analyzed 24 hours after transfection.

Fatty-acid analysis–Cells were cultured on 90-mm plastic dishes. After the chemical treatments, the cells were washed three times with DMEM containing 0.1% BSA without supplemental fatty acid, and then PBS was added. The cells were harvested by scraping, and then centrifuged at 500 g for 5 min. Precipitates were rapidly frozen in liquid nitrogen. Lipids were extracted by the method of Bligh and Dyer (31). Phospholipids were separated by thin-layer chromatography in 25:25:25:10:9 (v/v) chloroform: methyl acetate:1-propanol:methanol:0.25% KCl. The plates were sprayed with primulin, and the phospholipids were visualized under ultraviolet light. Spots corresponding to phosphatidylcholine (PC) were scraped off the plates, and the isolated PC was methylated with 1% H2SO4 in methanol. The resulting fatty-acid methyl esters were extracted with hexane and subjected to gas chromatography–mass spectrometry (GC-MS) analysis as described in Ariyama et al. (30).

Result

SCD1 inhibitor 28c suppresses starvation-induced autophagy–Novel autophagy inhibitor No. 73 has high structural similarity to a chemical that has been reported to be a SCD1 inhibitor: 4-Methyl-2-[4-[(*o*-tolylamino)methyl]benzoylamino] thiazole-5-carboxylic acid dimethylamide (24). Because this compound is not commercially available, I investigated whether another SCD1 inhibitor, 28c (27) (Fig. 3A), could suppress starvation-induced autophagy.

At a concentration of 20 μg/ml, 28c inhibited formation of GFP-LC3 puncta in

GFP-LC3 MEFs (Fig. 3B) and LC3 puncta in NIH3T3 and HeLa cells (Fig. 4A and B). The IC_{50} of 28c for inhibition of LC3 puncta formation in GFP-LC3 MEFs was ~2.0 μg/ml (~5.1 μM) (Fig. 3C). Similarly, this compound inhibited processing of LC3-I into LC3-II in GFP-LC3 MEFs (Fig. 3D, lanes 1–3), NIH3T3, and HeLa cells (Fig. 4C).

The inhibition of autophagy by No. 73 and 28c was reversible, as LC3 puncta appeared in the starvation medium after removal of either compound (Fig. 5).

I next examined the effects of baflomycin A_1, in order to exclude the possibility that 28c accelates degradation in autolysosomes and recycling of autolysosomes without inhibiting autophagosome formation. Bafilomycin A_1 inhibits degradation of content and recycling of autolysosomes (32). If 28c functions by accelerating degradation in autolysosomes and recycling of autolysosomes, bafilomycin A_1 would abolish the effects of 28c. As shown in Fig. 3D, the increase in the level of LC3-II after starvation was similarly suppressed by 28c treatment either in the presence or absence of bafilomycin A_1, suggesting that 28c inhibits formation of autophagosomes.

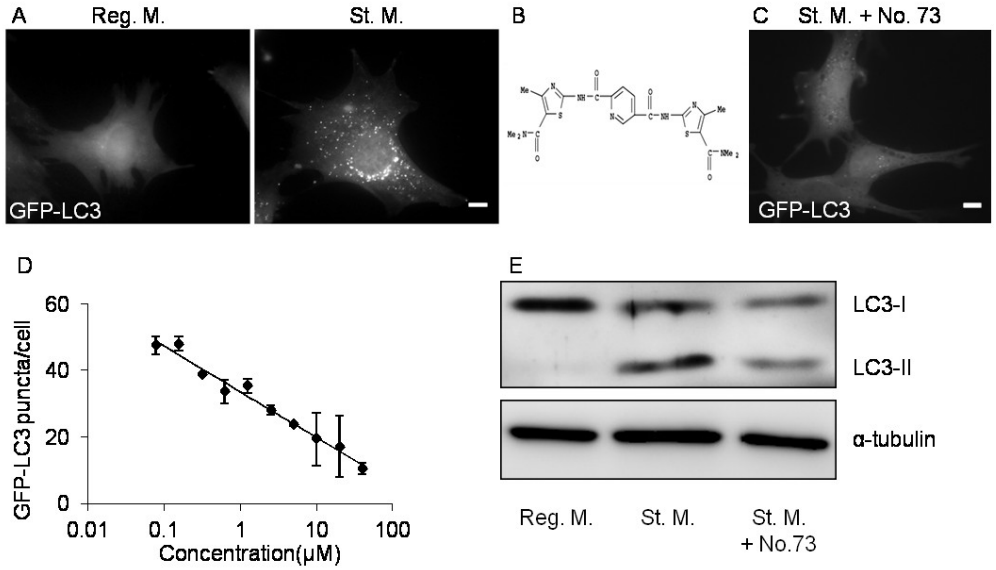

Figure 3. The SCD1 inhibitor 28c suppresses starvation-induced autophagy. (A) Structure of 28c. (B) GFP-LC3 MEFs were cultured for 2 h in starvation medium or starvation medium with 20 μg/ml 28c. Cells were observed under a fluorescence microscope. Scale bars, 10 μm. (C) Dose-dependent inhibition of autophagy by 28c. Numbers of GFP-LC3 puncta per cell were counted. Data represent means ± SE of three independent experiments, in each of which more than 30 cells were counted. (D) GFP-LC3 MEFs were cultured for 2 h in regular medium, starvation medium, or starvation medium with 20 μg/ml 28c, in the presence or absence of 100 nM bafilomycin A1. Cell lysates were processed for immunoblot analysis to detect LC3 and α-tubulin (as an endogenous control).

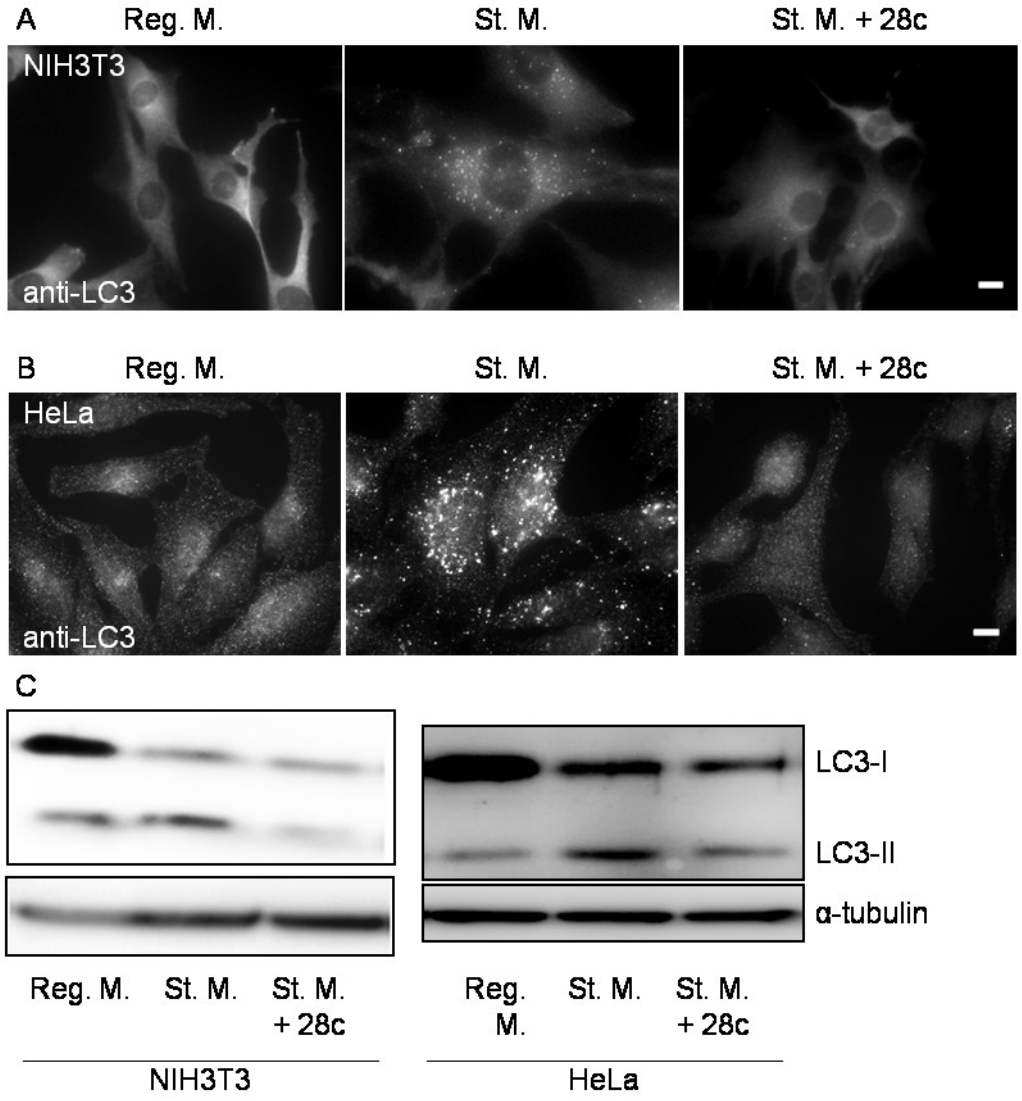

Figure 4. No. 73 and 28c suppress starvation-induced formation of LC3 puncta in NIH3T3 and HeLa cells. (A) NIH3T3 cells or (B) HeLa cells were cultured in regular medium (Reg. M.), starvation medium (St. M.), or starvation medium with 20 μg/ml 28c. Cells were processed for immunofluorescence microscopy with mouse monoclonal anti-LC3 antibody. Scale bars, 10 μm. (C) Immunoblot analysis of LC3 conversion from LC3-I to LC3-II in NIH 3T3 and HeLa cells. Samples were processed as in Figure 4A and B, and then analyzed by immunoblotting with anti-LC3 and anti–α -tubulin antibody (as an endogenous control).

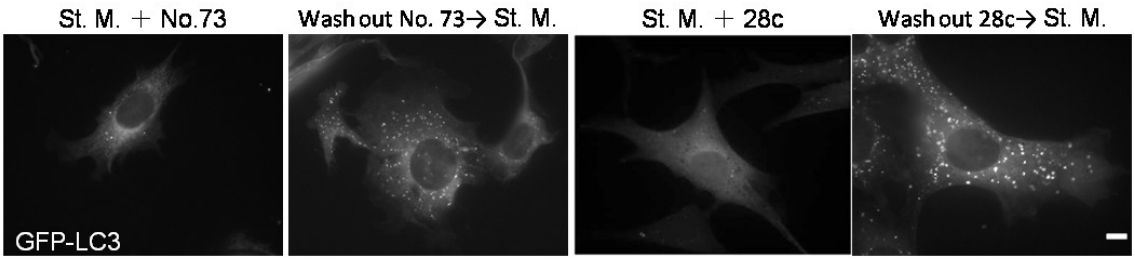

Figure 5. No. 73 and 28c are reversible inhibitors of autophagy. GFP-LC3 MEFs were cultured for 2 h in starvation medium with 20 μg/ml No. 73 or 20 μg/ml 28c. After the chemical was washed out, the cells were cultured for an additional 2 h in starvation medium. Scale bars, 10 μm.

28c suppresses autophagic degradation of p62/SQSTM1–p62/SQSTM1 binds to LC3, is specifically sequestered in autophagosomes, and is degraded in autolysosomes (33). Therefore, it has been used as a marker in studies of autophagic degradation (34)

As shown in Fig. 6A, the level of p62/SQSTM1 decreased during prolonged (8 h) starvation (lane 5), and this decrease was suppressed by 28c (lane 6). This result suggests that autophagy and degradation of p62/SQSTM1 was inhibited by 28c treatment.

Next, I measured the relative level of p62/SQSTM1 mRNA by quantitative PCR, in order to rule out the possibility that this observation was the result of upregulated synthesis of p62/SQSTM1 following 28c treatment. As reported by Sahani et al (29), the relative level of p62/SQSTM1 mRNA increased after prolonged starvation (Fig. 6B). However, 28c treatment itself did not affect the level of p62/ SQSTM1 mRNA (Fig. 6B).

I also examined changes in the level of exogenously expressed GFP-p62/ SQSTM1, because the rate of the synthesis of GFP-p62/SQSTM1 protein may not change in response to starvation or 28c treatment. Using exogenously expressed GFP-p62/SQSTM1, I obtained results similar to those obtained with endogenous p62/ SQSTM1 (Fig. 6A). These results strongly suggest that the suppression of the reduction in p62/SQSTM1 level during starvation in the presence of 28c is not caused by upregulation of the p62/SQSTM1 synthesis, and that 28c inhibits starvation-induced autophagy.

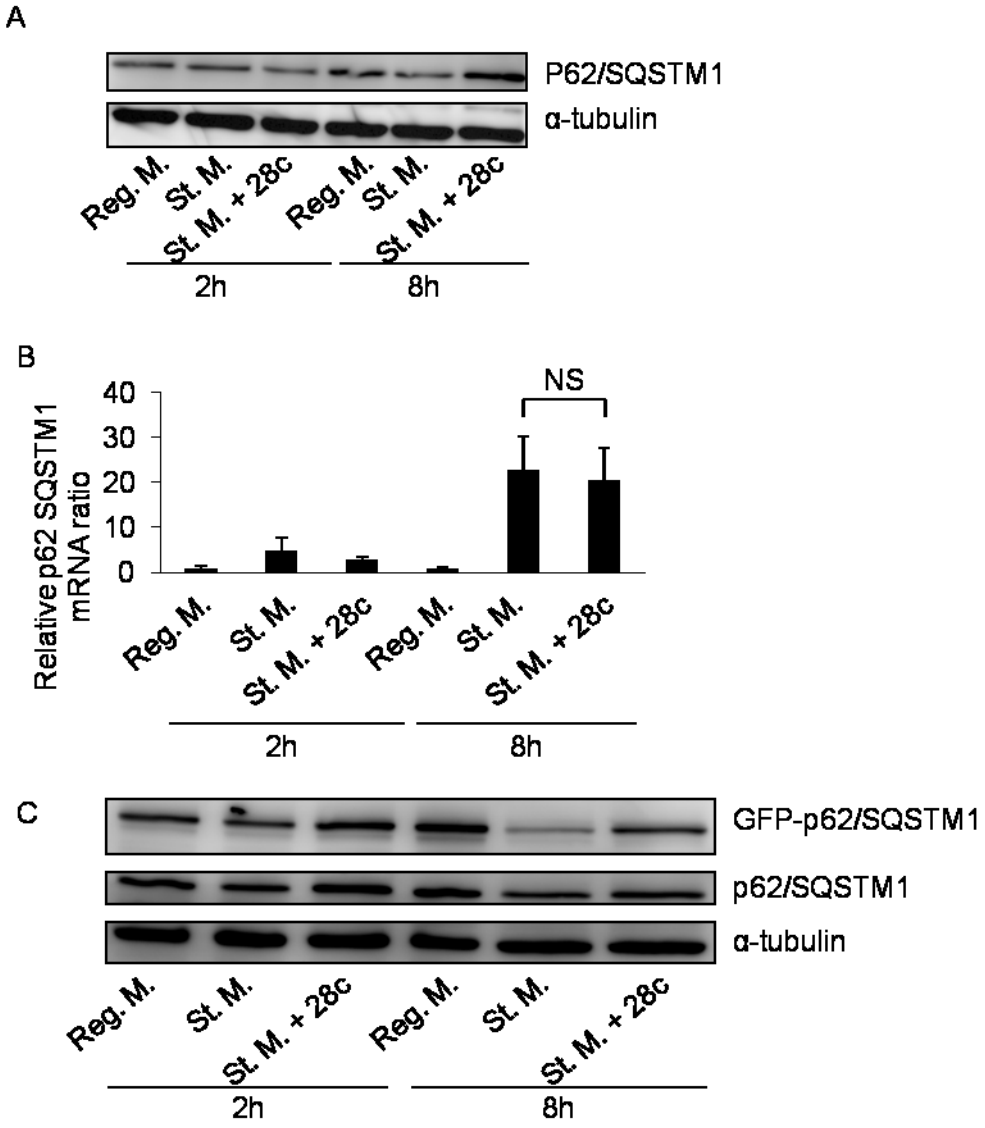

Figure 6. 28c inhibits starvation-induced degradation of exogenously expressed GFP-p62/SQSTM1. (A) GFP-LC3 MEFs were cultured for 2 h or 8 h in regular medium, starvation medium, or starvation medium with 20 μg/ml 28c. Cell lysates were processed for immunoblot analysis to detect p62/SQSTM1 and α-tubulin (as an endogenous control). (B) Quantitative PCR of p62/SQSTM1 mRNA and β-actin (Actb: as an internal control). Ratios of the levels of p62/SQSTM1 mRNA to Actb mRNA are shown. Data represent means ± SE of three independent experiments. NS., statistically not significant. (C) MEFs stably expressing GFP-p62 were cultured for 2 h or 8 h in regular medium, starvation medium, or starvation medium with 20 μg/ml 28c. Cell lysates were processed for immunoblot analysis to detect p62/SQSTM1, GFP and α-tubulin (as an endogenous control).

Electron-microscopic analysis of 28c treated cells–Next, I investigated the ultrastructure of 28c-treated cells. In regular medium, MEFs contained few autophagic structures in MEFs (Fig. 7A, Reg. M.). After nutrient deprivation, however, many autophagic structures appeared, including isolation membranes, autophagosomes, and autolysosomes (Fig. 7A, St. M.). By contrast, in the presence of 20 μg/ml 28c, few autophagic structures were observed even after starvation (Fig. 7A, St. M. + 28c). Fig. 7B shows quantitative analysis of the area of autophagic structures (autophagosomes and autolysosomes). 28c significantly suppressed formation of autophagic structures (Fig. 7B). Taken together with the results described above, these observations show that 28c inhibits starvation-induced autophagy, and suggest that SCD1 is required for autophagy.

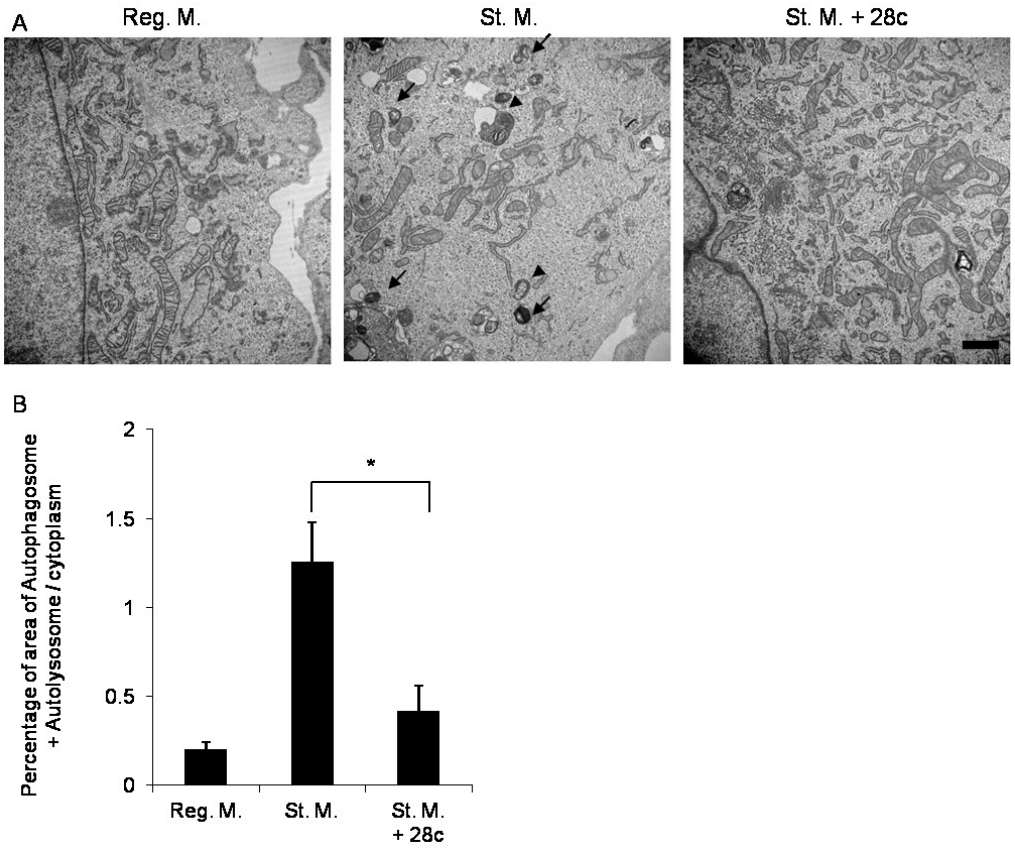

Figure 7. Electron-microscopic analysis of 28c-treated MEFs. (A) Electron micrographs of GFP-LC3 MEFs incubated for 2 h in regular medium, starvation medium, or starvation medium with 20 μg/ml 28c. Arrowheads indicate autophagosomes, and arrows show autolysosomes. Scale bars, 1 μm. (B) Quantitation of area of autophagosomes and autolysosomes. Data represent means ± SE of three independent experiments, in each of which more than 10 cells were counted. *, $p<0.05$

Overexpression of SCD1 abolishes inhibition of autophagy by 28c–To further investigate the involvement of SCD1 activity in autophagy, I asked knocked down SCD1 in HeLa cells. However, knockdown of SCD1 did not significantly suppress starvation-induced autophagy in HeLa cells (Fig. 8), possibly due to incomplete knockdown of SCD1 or redundant functions exerted by other SCD isozymes present in mammalian cells. Therefore, I next investigated whether overexpression of SCD1 abolishes inhibition of starvation-induced autophagy by 28c.

To this end, I constructed mammalian expression vectors (pEGFP-C2) encoding mouse SCD1 (GFP-SCD1) (Fig. 9A and B). The GFP-SCD1 fusion protein exhibits stearoyl-CoA desaturase activity similar to that of wild-type SCD1 (35). GFP-SCD1 expressed in NIH3T3 was co-localized with an endogenous ER protein, calnexin (Fig. 9C). NIH3T3 cells expressing GFP-SCD1 sometimes exhibited a punctate ER pattern in addition to the normal reticular pattern. This ER pattern did not change during starvation, and did not co-localize with LC3 puncta (Fig 10A right panel).

NIH3T3 cells transiently expressing GFP-SCD1 formed LC3 puncta after starvation, as in the case of the same cells expressing GFP alone (Fig. 10A, St. M.). In starvation medium containing 28c, overexpression of GFP-SCD1, but not GFP alone, restored LC3 puncta formation (Fig. 10A, St. M. + 28c). Fig. 10B shows the results of a quantitative analysis of LC3 puncta formation. Recovery of autophagy by overexpression of SCD1 was also demonstrated by immunoblot analyses in which processing from LC3-I into LC3-II was detected (Fig. 10C, Lane 5 and 6).

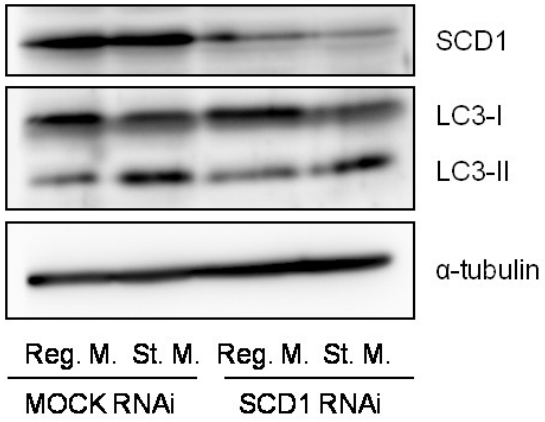

Figure 8. Knockdown of SCD1 does not significantly suppress starvation-induced autophagy. Seventy-two hours after transfection with siRNA against SCD1 (SCD1 RNAi) or mock transfection (MOCK RNAi), HeLa cells were cultured for 2 h in regular or starvation medium. Cell lysates were processed for immunoblot analysis for SCD1, LC3, and α-tubulin (as an endogenous control).

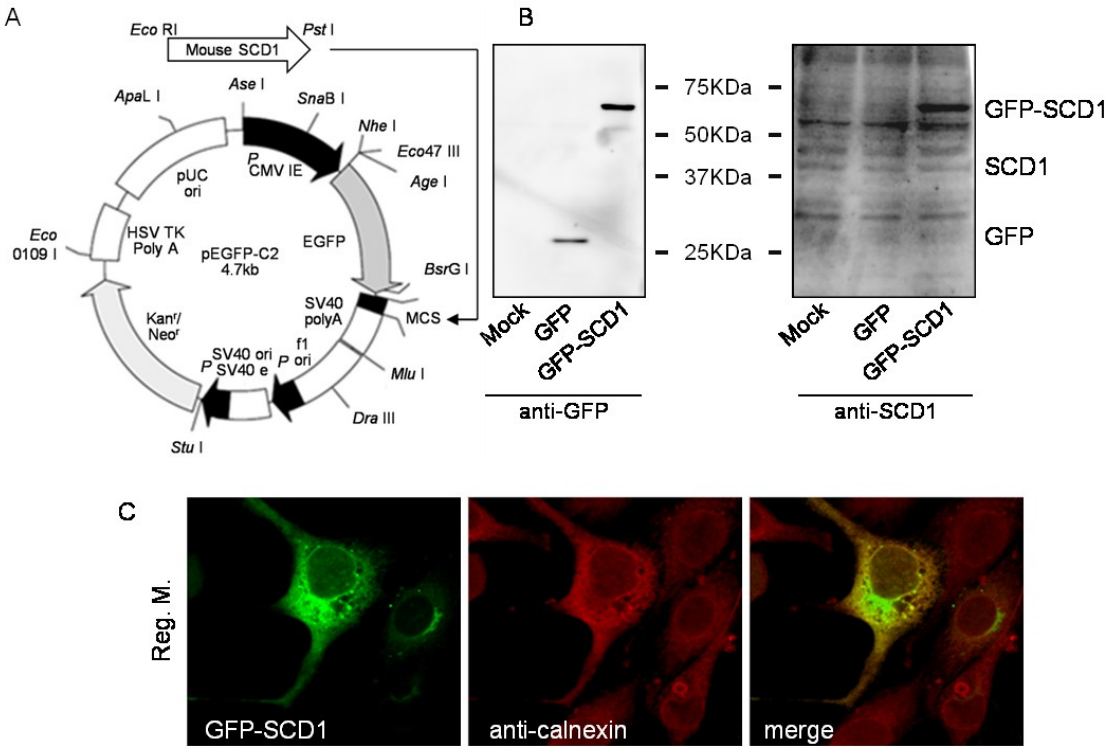

Figure 9. Overexpression of GFP-SCD1. (A) Cloned SCD1 cDNA from NIH3T3 cells was ligated into vector pEGFP-C2. (B) NIH3T3 (Mock) cells and NIH3T3 cells transiently expressing GFP-SCD1 (GFP-SCD1) or GFP (GFP) were lysed and subjected to immunoblot analysis to detect SCD1 and GFP. (C) NIH3T3 cells transiently expressing GFP-SCD1 were fixed, permeabilized, and subjected to immunofluorescence confocal microscopy to detect calnexin.

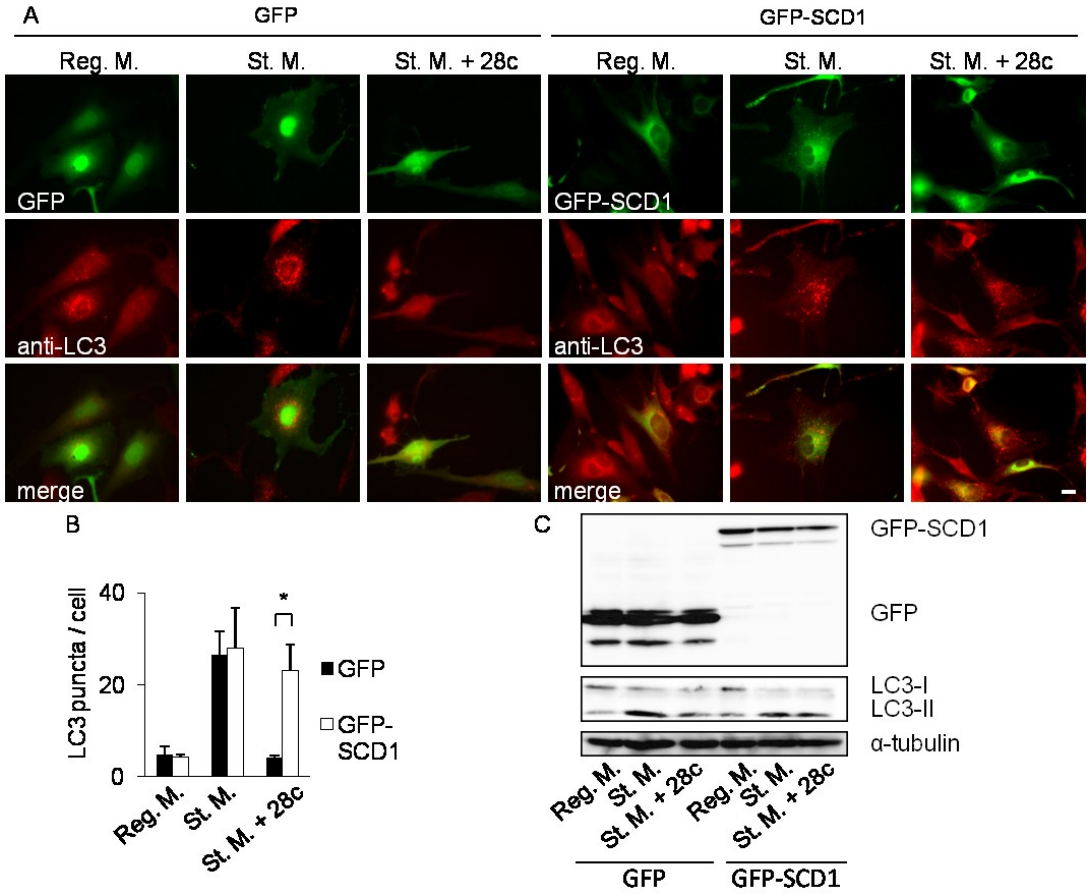

Figure 10. Overexpression of GFP-SCD1 abolishes the effect of 28c. (A) NIH3T3 cells transiently expressing GFP (left panel) or GFP-SCD1 (right panel) were cultured for 2 h in regular medium, starvation medium, or starvation medium with 20 μg/ml 28c. Cells were processed for immunofluorescence microscopy with mouse monoclonal anti-LC3 antibody and Alexa Fluor 546–conjugated secondary antibody. Upper panels; GFP, middle panels; LC3, lower panels; merge. Scale bars, 10 μm. (B) Numbers of LC3 puncta per cell were counted. Data represent means ± SE of three independent experiments, in each of which more than 20 cells were counted. *, $p < 0.05$. (C) NIH3T3 cells transiently expressing GFP or GFP-SCD1 were cultured for 2 h in regular medium, starvation medium, or starvation medium with 20 μg/ml 28c. Cell lysates were processed for immunoblot analysis to detect GFP, LC3, and α-tubulin (as an endogenous control).

LC3 puncta formation in the presence of 28c is restored by oleic acid supplementation–SCD1 catalyzes synthesis of mono-unsaturated fatty acids (MUFA) from saturated fatty acids (SFA). The main product of SCD1 is oleic acid (OA), which

is synthesized from stearic acid by desaturation. Therefore, I investigated whether exogenous supplementation of oleic acid restores autophagy in the presence of 28c.

First, I examined the changes in fatty-acid composition of phosphatidylcholine resulting from 28c treatment or oleic acid supplementation. 28c treatment decreased oleic acid composition slightly (Fig. 11A, 18:1n-9) both in regular and starvation medium, although these reductions were not significant. These results show that the overall lipid composition of whole cells did not change dramatically following short (2 h) treatment with 28c. On the other hand, supplementation with oleic acid (Fig. 11A) resulted in a significant increase in oleic acid (18:1n-9) incorporation in phosphatidylcholine. Similar results were obtained for the ratio of MUFA to SFA (Fig. 11B).

Next, I investigated whether oleic acid supplementation would abolish the effect of 28c. Supplementation of regular or starvation medium with 500 μM OA-BSA conjugate did not change the distribution of LC3 (Fig. 12A Reg. M. + OA and St. M. + OA). Addition of 500 μM OA-BSA conjugate to starvation medium containing 28c restored LC3 puncta formation (Fig. 12A St. M. + 28c + OA). On the other hand, vehicle control (1.25% BSA) did not abolish the effect of 28c (Fig. 12A St. M. + 28c + BSA). Fig. 12B shows quantitative analyses of LC3 puncta formation. Furthermore, addition of 100 μM PA-BSA conjugate to starvation medium containing 28c did not restore LC3 puncta formation (Fig. 13). Taken together, these results strongly suggest that 28c suppresses starvation-induced autophagy by inhibiting SCD1 activity, but that SCD1 activity is required for autophagy at specific locations, such as autophagosome formation sites.

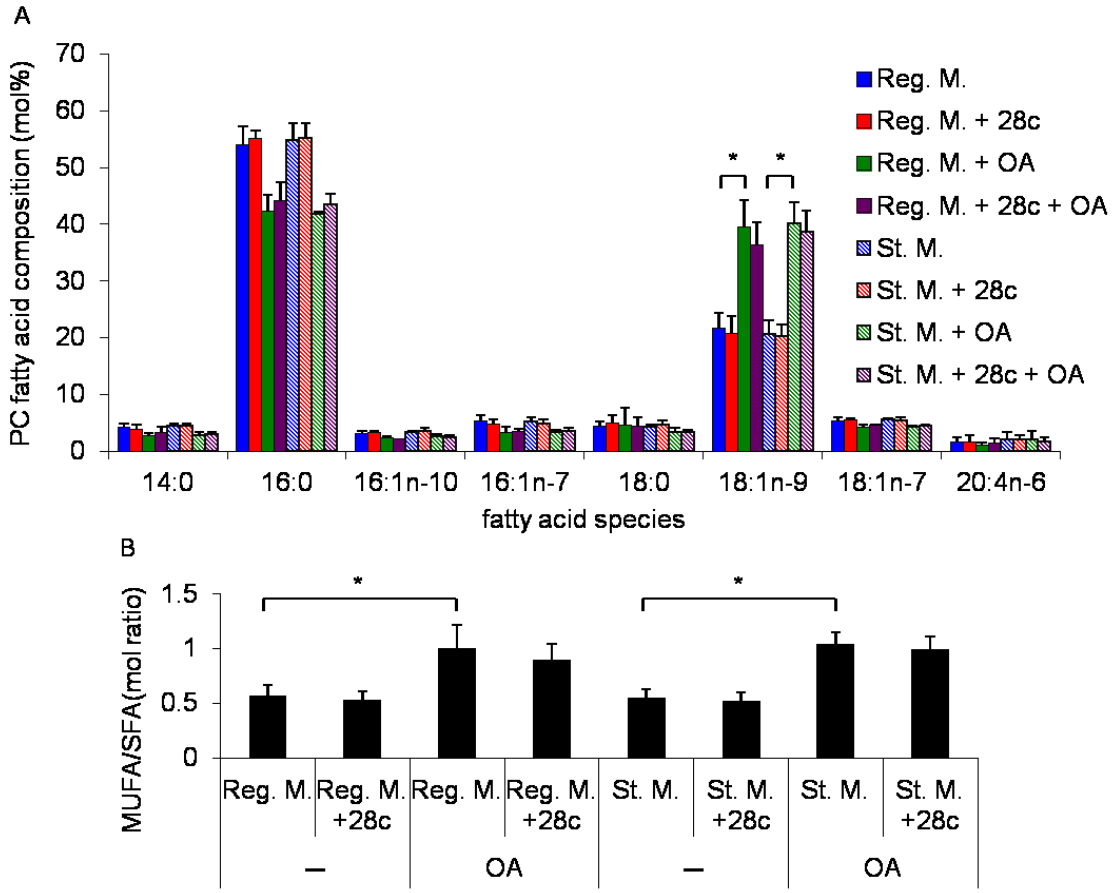

Figure 11. Changes of fatty-acid composition in phosphatidylcholine (PC) following 28c treatment or addition of oleic acid. GFP-LC3 MEFs were cultured for 2 h in regular or starvation medium, with or without 20 μg/ml 28c, in the presence or absence of 500 μM OA-BSA conjugate (OA). Fatty-acid composition of the harvested cells was analyzed by GC/MS. Data represent means ± SE of three or more independent experiments. (A) Molar percentages of fatty-acid species in PC. (B) Ratio of molar percentage of monounsaturated fatty acid (MUFA) to saturated fatty acid (SFA) in Figure 11A. *, $p < 0.01$.

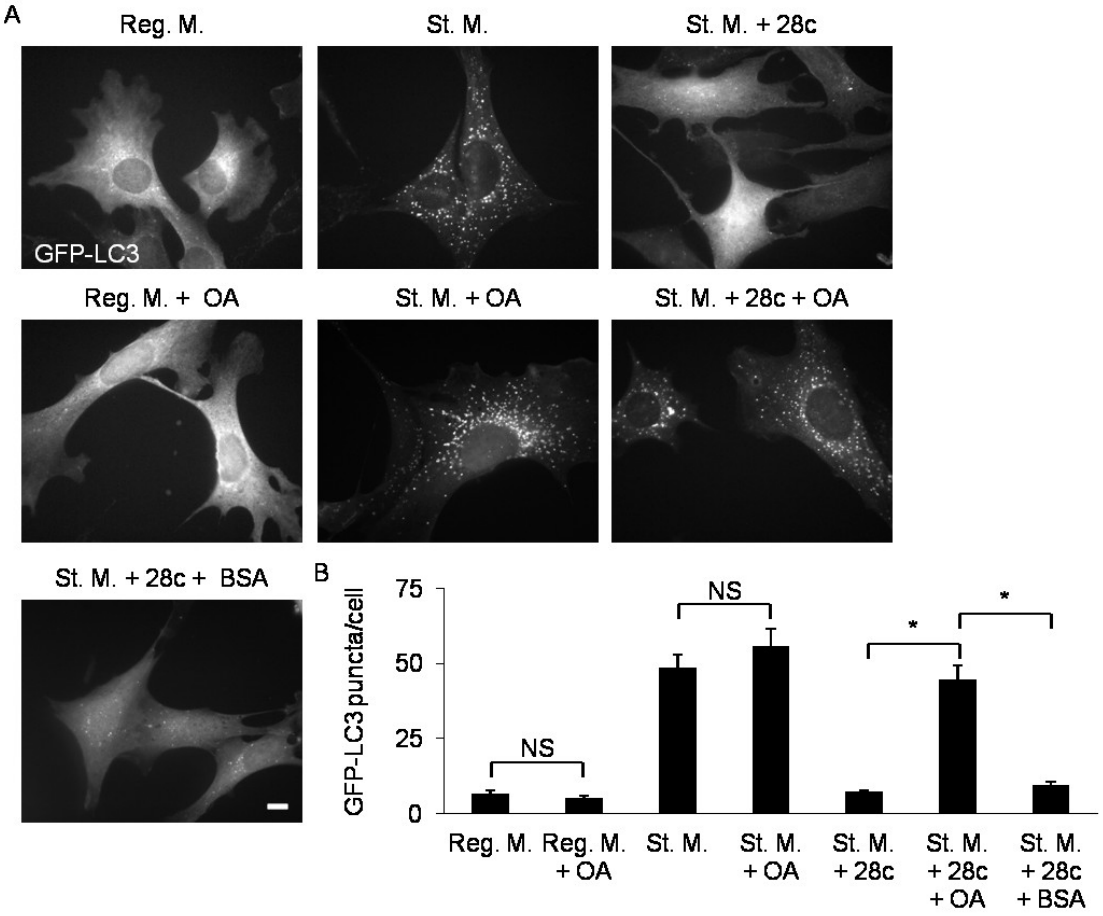

Figure 12. Supplementation of oleic acid abolishes the effect of 28c. (A) GFP-LC3 MEFs were cultured for 2 h in regular or starvation medium, with or without 500 μM OA-BSA conjugate (OA), or in St. M. with 20 μg/ml 28c in the presence or absence of 500 μM OA-BSA conjugate or 1.25% BSA. Cells were observed under a fluorescence microscope. Scale bars, 10 μm. (B) Numbers of GFP-LC3 puncta per cell were counted. Data represent means ± SE of three independent experiments, in each of which more than 30 cells were counted. NS., statistically not significant;*, $p < 0.01$.

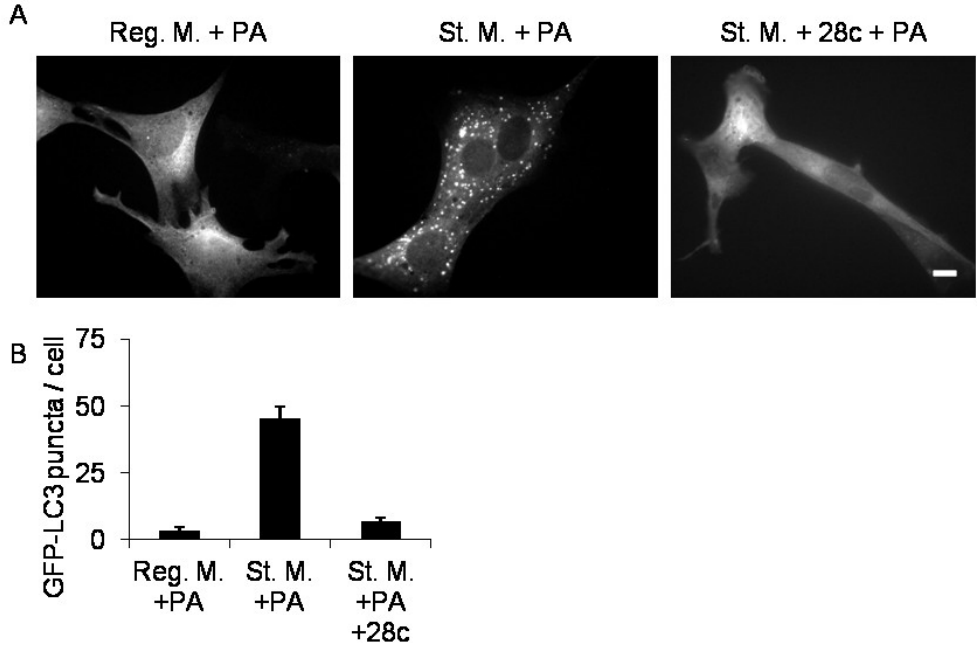

Figure 13. Palmitic acid did not restore starvation-induced autophagy in the presence of 20 μg/ml 28c. (A) GFP-LC3 MEFs were cultured for 2 h in regular medium (Reg. M), starvation medium (St. M.), or St. M. with 20 μg/ml 28c in the presence of 100 μM PA-BSA conjugate. Cells were observed under a fluorescence microscope. Scale bars, 10 μm. (B) Numbers of GFP-LC3 puncta per cell were counted. Data represent means ± SE of three independent experiments, each of which counted more than 50 cells.

28c suppresses starvation-induced autophagy downstream of mTOR– Mammalian target of rapamycin (mTOR) plays a central role in signal transduction in response to nutrient conditions. Under nutrient-rich conditions, mTOR suppresses autophagy via phosphorylation of ULK1. Following nutrient deprivation, however, mTOR is inactivated and ULK1 is dephosphorylated, resulting in induction of autophagy.

Rapamycin, a potent mTOR inhibitor, induces autophagy directly without starvation. To determine whether 28c suppresses the signal transduction pathway leading to mTOR, I investigated whether 28c suppresses rapamycin-induced autophagy. 28c strongly suppressed GFP-LC3 puncta formation (Fig. 14A, B) and conversion of LC3-I into LC3-II (Fig. 14C) upon rapamycin treatment. These results suggest that 28c suppresses autophagy downstream of mTOR.

Next, I investigated whether mTOR activity is activated in 28c-treated cells. To

monitor mTOR activity, I examined phosphorylation of ribosomal protein S6, which is a target of the mTOR kinase (36). In regular medium, S6 was phosphorylated by mTOR, whereas S6 phosphorylation decreased after starvation. Although starvation-induced autophagy was suppressed by 28c treatment, S6 remained dephosphorylated (Fig. 14D). This result suggests that 28c does not suppress inactivation of mTOR activity in starvation medium.

I also investigated whether AMPK is suppressed by 28c treatment. Depletion of energy causes activation of AMPK by AMPK kinase. Activated AMPK then phosphorylates and activates ULK1, resulting in induction of autophagy (37). To determine whether 28c suppresses this second pathway for induction of autophagy, I examined the effects of 28c on the phosphorylation of AMPK after starvation (Fig. 14E). The results showed that 28c did not suppress AMPK phosphorylation, demonstrating that 28c does not inhibit the activation of AMPK by phosphorylation after starvation. Taken together, these results show that 28c suppresses autophagy downstream of mTOR.

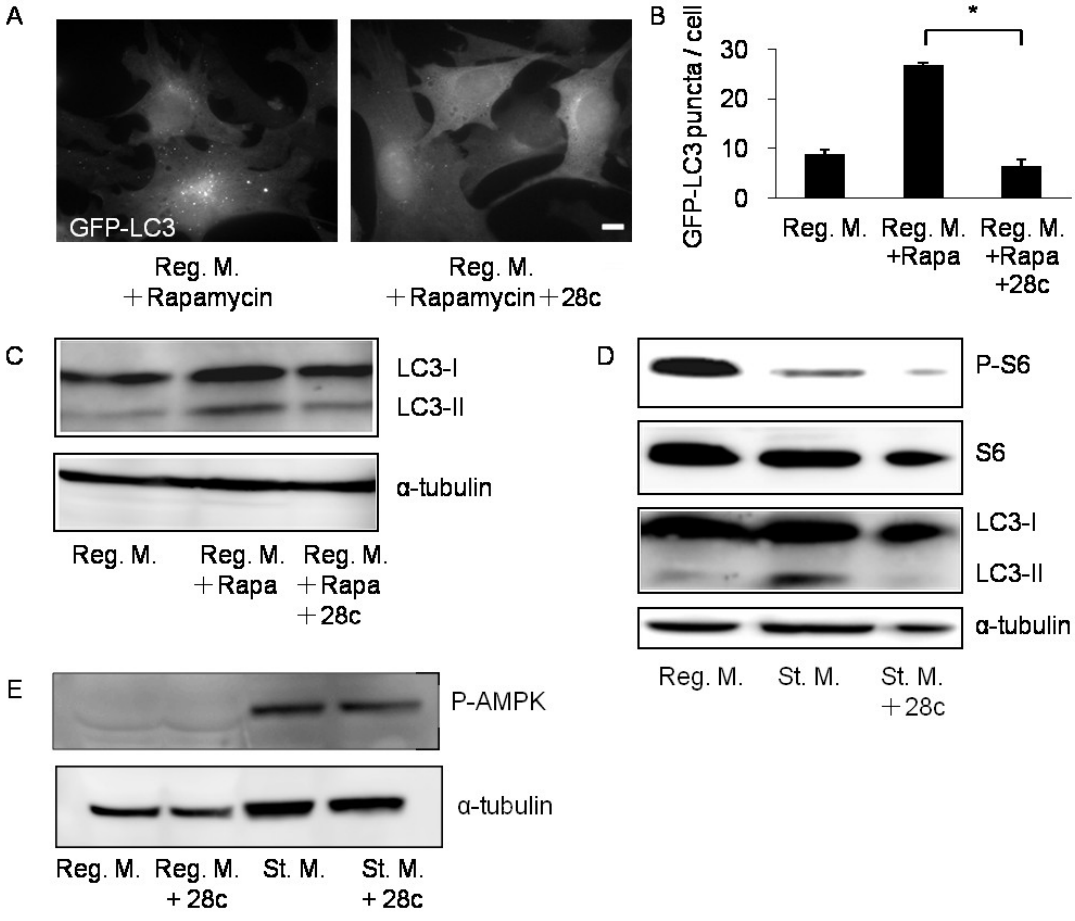

Figure 14. 28c suppresses rapamycin-induced autophagy. (A) GFP-LC3 MEFs were cultured for 2 h in regular medium with 1 μM rapamycin or 1 μM rapamycin and 20 μg/ml 28c. Cells were observed under a fluorescence microscope. Scale bars, 10 μm. (B) Number of GFP-LC3 puncta per cell were counted. Data represent means ± SE of three independent experiments, in each of which more than 100 cells were counted. *, $p < 0.01$. (C) NIH3T3 cells were cultured for 2 h in regular medium with no drug, with 1 μM rapamycin, or with 1 μM rapamycin and 20 μg/ml 28c. Cell lysates were processed for immunoblot analysis to detect LC3 and α-tubulin (as an endogenous control). (D) NIH3T3 cells were cultured for 2 h in regular medium, starvation medium, or starvation medium with 20 μg/ml 28c. Cell lysates were processed for immunoblot analysis to detect phospho-S6 (P-S6), S6, LC3, and α-tubulin (as an endogenous control). Rapa, rapamycin. (E) NIH3T3 cells were cultured for 2 h in regular medium or starvation medium, with or without 20 μg/ml 28c. Cell lysates were processed for immunoblot analysis to detect phospho-AMPKα and α-tubulin (as an endogenous control).

28c suppresses autophagy at the earliest step of autophagosome formation–During autophagosome formation, ULK1, WIPI1, Atg16L, and LC3 target sites of autophagosome formation on the ER and form puncta in a hierarchical manner in the listed order (20).

To determine which step is inhibited by 28c, I investigated the effects of 28c on the localization of ULK1, WIPI1, and Atg16L under starvation conditions. MEFs stably expressing GFP-ULK1 or GFP-WIPI1 formed fluorescent puncta after starvation (Fig. 15A and C, St. M.). Formation of endogenous Atg16L puncta was detected by immunofluorescence microscopy (Fig. 15A, St. M.). Formation of puncta containing ULK1, WIPI1, and Atg16L were inhibited by addition of 28c to the starvation medium (Fig. 15A and C, St. M + 28c). Fig. 15B and D show the results of quantitative analyses of formation of ULK1, WIPI1, and Atg16L puncta. Formation of all types of puncta was suppressed by 28c treatment, suggesting that 28c inhibits the earliest step of autophagosome formation, namely, translocation of ULK1 to sites of autophagosome formation on the ER.

I next examined whether OA supplementation restores puncta formation of ULK1 in 28c treated cells. As shown Fig. 15C, supplementation of media with OA-BSA conjugate restored starvation-induced formation of ULK1 puncta even in the presence of 28c. Fig. 15D shows the results of quantitative analyses of formation of GFP-ULK1 puncta. These observations suggest that unsaturated fatty acids produced by SCD1 are required for translocation of ULK1 to sites of autophagosome formation.

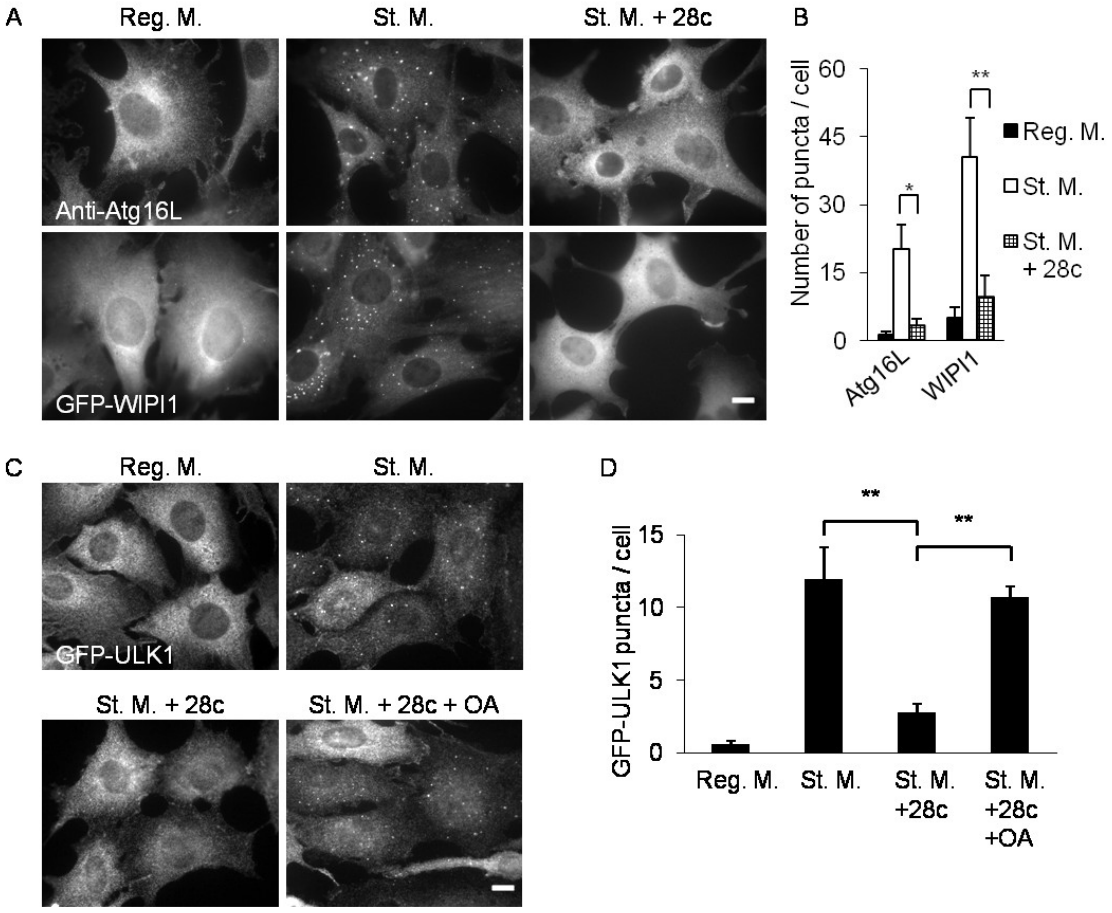

Figure 15. 28c suppresses starvation-induced autophagy in the early stage of autophagosome formation. (A) MEFs stably expressing GFP-LC3 (upper panels) and GFP-WIPI1 (lower panels) were cultured for 2 h in regular medium, starvation medium, or starvation medium with 20 μg/ml 28c. Cells were fixed and observed under a fluorescence microscope either directly (lower panels) or after immunostaining with anti-Atg16L antibody (upper panels). Scale bars, 10 μm. (B) Numbers of Atg16L and WIPI1 puncta per cell were counted. Data represent means ± SE of three independent experiments, in each of which more than 100 cells were counted. (C) MEFs stably expressing GFP-ULK1 were cultured for 2 h in regular medium, starvation medium, or starvation medium with 20 μg/ml 28c in the presence or absence of 500 μM OA-BSA conjugate. Cells were fixed and observed under a fluorescence microscope after immunostaining with anti-GFP antibody. Scale bars, 10 μm. (D) Numbers of GFP-ULK1 puncta per cell were counted. Data represent means ± SE of three independent experiments, in each of which more than 100 cells were counted. *, $p < 0.05$; **, $p < 0.01$. .

28c inhibits translocation of p62/SQSTM, but not Atg9–Next, I investigated the effects of 28c on the localization of p62/SQSTM1 and Atg9, both of which act early in autophagosome formation. p62/SQSTM1 is the best-characterized specific substrate of mammalian autophagy (34). Recent work has shown that p62/SQSTM1 translocates to sites of autophagosome formation after starvation, regardless of the presence or absence of ULK1 complex (38).

Under nutrient-rich conditions, p62/SQSTM1 scarcely formed puncta, whereas following starvation, it formed many puncta (Fig. 16A). In the presence of 28c, p62/SQSTM1 did not form puncta after starvation, but addition of 500 μM OA-BSA conjugate to starvation medium containing 28c restored p62/SQSTM1 puncta formation (Fig. 16A). Fig. 16B shows the results of quantitative analyses of formation of p62/SQSTM1 puncta.

Atg9 is the only known transmembrane protein among the autophagy-related proteins, and it localizes both in the trans-Golgi network (juxtanuclear region) and in the peripheral region, including late endosomes (39). A recent study showed that Atg9 translocates to the peripheral region from the juxtanuclear region, and transiently interacts with omegasomes under starvation conditions (40). 28c did not suppress the Atg9's shift in localization from the juxtanuclear region to the periphery after starvation (Fig. 16C and D)

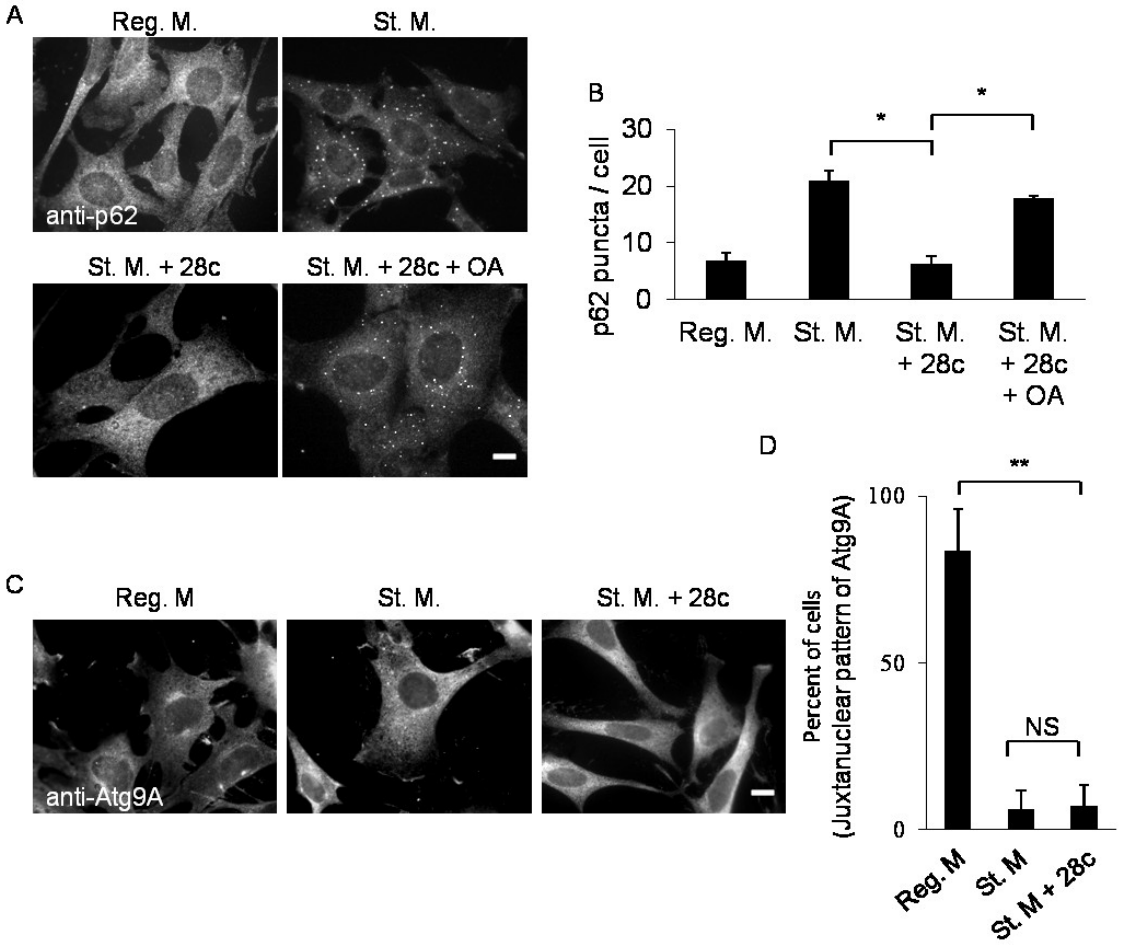

Figure 16. 28c inhibits formation of p62/SQSTM1 puncta, but does not affect the change in Atg9 localization from a juxtanuclear to a peripheral pattern. (A) GFP-LC3 MEFs were cultured for 2 h in regular medium, starvation medium, or starvation medium with 20 μg/ml 28c in the presence or absence 500 μM OA-BSA conjugate. Cells were processed for immunofluorescence microscopy with anti-p62/SQSTM1 antibody. Scale bars, 10 μm. (B) Numbers of p62/SQSTM1 puncta per cell were counted. Data represent means ± SE of three independent experiments, in each of which more than 50 cells were counted. (C) GFP-LC3 MEFs were cultured for 2 h in regular medium, starvation medium, or starvation medium with 20 μg/ml 28c. Cells were processed for immunofluorescence microscopy to detect Atg9A. Scale bars, 10 μm. (D) Percent of cells exhibiting a juxtanuclear pattern of Atg9A. Data represent means ± SE of three independent experiments, in each of which more than 30 cells were counted. NS., statistically not significant; *, $p < 0.05$; **, $p < 0.01$.

Discussion

One of the effective inhibitors that I identified has a structure similar to that of a chemical previously described as an SCD1 inhibitor. Another SCD1 inhibitor, 28c, also inhibited starvation-induced autophagy, suggesting that SCD1 activity is necessary for autophagy. As noted above, autophagy is suppressed by knock-out of a Drosophila SCD homolog, Desat1 (25). My findings reported here constitute the first demonstration that SCD is required for autophagy in mammals.

In this study, I demonstrated that inhibition of starvation-induced autophagy by 28c is abolished by either addition of oleic acid or overexpression of SCD1. This result strongly suggests that inhibition of starvation-induced autophagy by 28c is caused by inhibition of SCD1 activity, and is not a side effect of the drug. In HepG2 cells, the IC_{50} of 28c for in vivo SCD1 activity is 7–8 nM, and 28c almost completely inhibits SCD1 activity at a concentration of 1 μM (27). In this study, the IC_{50} of 28c for starvation-induced autophagy was ~5.1 μM, much higher than the concentration required to inhibit SCD1 activity. This difference between the IC_{50} for SCD1 activity and the IC_{50} for inhibition of autophagy might be explained by the presence of SCD isozymes that are more resistant than SCD1 to 28c and that also participate in autophagy. It is also possible that residual SCD1 activity in the presence of nanomolar concentrations of 28c is sufficient for autophagy. 28c suppressed starvation-induced autophagy without affecting inactivation of mTOR after nutrient deprivation, and also suppressed rapamycin-induced autophagy, suggesting a requirement for SCD1 activity downstream of mTOR. Following starvation, 28c inhibited formation of puncta containing p62/ SQSTM1, ULK1, WIPI1, and Atg16L, as well as LC3. Formation of ULK1 and p62/SQSTM1 puncta is the earliest step of autophagosome formation, corresponding to the targeting of these proteins to the ER followed by construction of omegasomes (sites of autophagosome formation) on the ER. Supplementation with oleic acid restored ULK1 and p62/SQSTM1 puncta formation, suggesting that a MUFA such as oleic acid may be indispensable for the earliest step of autophagosome formation.

Reference

26. Paton, C. M., Ntambi, J. M. (2009) Biochemical and physiological function of stearoyl-CoA desaturase. Am J Physiol Endocrinol Metab. 297, 28-37
27. Liu, G., Lynch, J. K., Freeman, J., Liu, B., Xin, Z., Zhao, H., Serby, M. D., Kym, P. R., Suhar, T. S., Smith, H. T., Cao, N., Yang, R., Janis, R. S., Krauser, J. A., Cepa, S. P., Beno, D. W., Sham, H. L., Collins, C. A., Surowy, T. K., Camp, H. S. (2007)

Discovery of potent, selective, orally bioavailable stearoyl-CoA desaturase 1 inhibitors. J Med Chem. 50, 3086-3100

28. Hannah, V. C., Ou, J., Luong, A., Goldstein, J. L., Brown, M. S. (2001) Unsaturated fatty acids down-regulate srebp isoforms 1a and 1c by two mechanisms in HEK-293 cells. J Biol Chem. 276, 4365-4372
29. Sahani, M.H., Itakura, E., Mizushima, N. (2014) Expression of the autophagy substrate SQSTM1/p62 is restored during prolonged starvation depending on transcriptional upregulation and autophagy-derived amino acids. Autophagy. 10, 431-441.
30. Ariyama, H., Kono, N., Matsuda, S., Inoue, T., Arai, H. (2010) Decrease in membrane phospholipid unsaturation induces unfolded protein response. J Biol Chem. 285, 22027-22035
31. Bligh, E. G., Dyer, W. J. (1959) A rapid method of total lipid extraction and purification. Can J Biochem Physiol. 37, 911-917
32. Barth, S., Glick, D., Macleod, K. F. (2010) Autophagy: assays and artifacts. J Pathol. 221, 117–124
33. Bjørkøy, G., Lamark, T., Brech, A., Outzen, H., Perander, M., Overvatn, A., Stenmark, H., Johansen, T. (2005) p62/SQSTM1 forms protein aggregates degraded by autophagy and has a protective effect on huntingtin-induced cell death. J Cell Biol. 171, 603-614
34. Bjørkøy, G., Lamark, T., Pankiv, S., Øvervatn, A., Brech, A., Johansen, T. (2009) Monitoring autophagic degradation of p62/SQSTM1. Methods Enzymol. Autophagy in Mammalian Systems, Part B. 452, 181-197
35. Wang, J., Yu, L., Schmidt, R. E., Su, C., Huang, X., Gould, K., Cao, G. (2005) Characterization of HSCD5, a novel human stearoyl-CoA desaturase unique to primates. Biochem Biophys Res Commun. 332, 735-742
36. Martin, D. E., Hall, M. N. (2005) The expanding TOR signaling network. Curr Opin Cell Biol. 17, 158-166
37. Egan, D. F., Shackelford, D. B., Mihaylova, M. M., Gelino, S., Kohnz, R. A., Mair, W., Vasquez, D. S., Joshi, A., Gwinn, D. M., Taylor, R., Asara, J. M., Fitzpatrick, J., Dillin, A., Viollet, B., Kundu, M., Hansen, M., Shaw, R. J. (2011) Phosphorylation of ULK1 (hATG1) by AMP-activated protein kinase connects energy sensing to mitophagy. Science. 33, 1456-1461
38. Itakura, E., Mizushima, N. (2011) p62 Targeting to the autophagosome formation site requires self-oligomerization but not LC3 binding. J Cell Biol. 192, 17-27
39. Young, A. R., Chan, E. Y., Hu, X. W., Köchl, R., Crawshaw, S. G., High, S.,

Hailey, D. W., Lippincott-Schwartz, J., Tooze, S. A. (2006) Starvation and ULK1-dependent cycling of mammalian Atg9 between the TGN and endosomes. J Cell Sci. 119, 3888-3900

40. Orsi, A., Razi, M., Dooley, H. C., Robinson, D., Weston, A. E., Collinson, L. M., Tooze, S. A. (2012) Dynamic and transient interactions of Atg9 with autophagosomes, but not membrane integration, are required for autophagy. Mol Biol Cell. 23, 1860-1873

Chapter IV. Yeast genetic analysis of the necessity of fatty acid desaturation for autophagy.

Abstract

As described above, SCD1 activity is required in mammalian autophagy. For further elucidating the role of SCD1, I used *Saccharomyces cerevisiae* (S. cerevisiae) as a model system. *S. cerevisiae* is a good model for defining of importance of fatty acid desaturation in autophagy because molecular mechanism of autophagy is clearer than that of mammals and contents of unsaturated fatty acid in cells can be significantly decreased by deficient of *OLE1*which is yeast homolog of SCD1. The *ole1* mutants did not show nitrogen starvation-induced autophagy and intracellular transport by cytoplasm to vacuole targeting (Cvt) pathway, in alkaline phosphatase (ALP) assay and Ape1 assay, respectively. These result clearly indicated that fatty acid desaturation is universally required for the autophagy in eukaryote cells.

Introduction

I demonstrated that SCD1 activity is required at the earliest step of autophagosome formation in mammalian autophagy. For further elucidating the role of SCD1, I tried knockdown of SCD1 in HeLa cells. Unfortunately, I was unable to clearly show that knockdown of SCD1 suppresses autophagy, possibly because other SCD isozymes exert redundant functions in mammalian cells. In fact, SCD4 mRNA is upregulated to compensate for SCD1 deficiency in the hearts of SCD1 KO mice (41).

Therefore, next, I used *S. cerevisiae* as a model system. *S. cerevisiae* is a good model for defining of importance of fatty acid desaturation in autophagy, because molecular mechanism of autophagy is clearer than that of mammals, and Stukey et al. reported that synthesis of unsaturated fatty acid is inhibited by deficient of *OLE1* which is only yeast homolog of SCD1 (42).

In this study, I constructed *ole1* mutants which are inserted the *Candida glabrata HIS3* (*CgHIS3*) in the *OLE1* locus, and investigated whether autophagic activity after nitrogen starvation and intracellular transport by cytoplasm to vacuole targeting (Cvt) pathway under nutrient rich condition are inhibited. For measurement of autophagic activity, I used *pho8Δ60* strains. Alkaline phosphatase, Pho8 is the vacuolar membrane protein and synthesized in ER as inactive form, and then transited from ER to the vacuole through a potion of the secretory pathway. In the vacuole, C-terminal peptide of Pho8 is removed by vacuolar protease Pep4 and become active form. Pho8Δ60 which is genetically deleted N-terminal 60 amino acid residues corresponding to transmembrane domain of Pho8 becomes soluble and is dispersed throughout the cytoplasm as an

inactive enzyme. Pho8Δ60 is nonselectively sequestered and delivered to the vacuole by autophagosome after nitrogen starvation. Therefore, alkaline phosphatase (ALP) activity in a pho8Δ60 strains corresponds to autophagic activity (43). I also investigated whether Cvt pathway is suppressed in *ole1* mutants. Cvt pathway is a highly selective process of autophagy and transports the resident vacuolar hydrolases, aminopeptidase I (Ape1) from cytoplasm to vacuole in nutrient-rich condition (44). Ape1 is synthesized as a precursor form (prApe1) in cytoplasm and processed as mature form (mApe1) by cleavage of the propeptide of prApe1in vacuole. Therefore, activity of Cvt pathway is examined by compare amounts of prApe1 and mApe1. As a result, I demonstrated that The *ole1* mutants did not show nitrogen starvation-induced autophagy and intracellular transport by Cvt pathway, in ALP and Ape1 assay, respectively. These result clearly indicated that fatty acid desaturation is universally required for the autophagy in eukaryote cells.

Experimental procedures

Yeast strains and culture–The yeast strains used in this study are listed in Table I. The cells were grown in YPD medium (1% yeast extract, 2% peptone, 2% glucose) or YPD medium containing 1mM oleic acid and 1% tritonX-100 (YPD + OA) at 30 °C. To induce autophagy, the cells in log phase were grown in YPD medium for 2h to deplete monounsaturated fatty acid in *ole1* deficient cells (42), and then incubated in SD(-N) medium (0.17% yeast nitrogen base without ammonium sulfate and amino acids, and with 2% glucose) or YPD medium containing 500 nM rapamycin for 3h.

Protein extraction from yeast cells–2 OD_{600} units of cells were collected and resuspended in 100 μl of 0.2M NaOH containing 1% β-mercaptoethanol. The cells were incubated on ice for 10 min and added 1ml of ice-cold acetone and then incubated on ice for 10min. After centrifugation at 20,000 g for 10 min at 4 °C, the resulting pellets were added 1ml of ice-cold acetone and cracked by sonication. After centrifugation at 20,000 g for 10 min at 4 °C, the resulting pellets were added 100 μl of cracking buffer : 8M urea, 5% SDS, 40mM Tris-HCl (pH 6.8), and sonicated completely. The sonicated solution were added 1 μl of β-mercaptoethanol and quite small amount of BPB solution and then boiled for 5min at 100 °C. Protein contents of cell lysates were determined by RCDC assay and equal amounts of protein (30 μg) were processed for Immuno-blot analysis. The Ape1 was detected by rabbit anti-Ape1 antibody. Rabbit anti-Ape1 anti body was kindly provided by Professor Takeshi Noda (Osaka University, Osaka)

Monitoring autophagic activity in yeast cells–Autophagic activity was measured by ALP assay. 1 OD_{600} unit of the cells were collected after autophagy induction, and

washed thrice with ice-cold assay buffer (250 mM Tris-HCl, pH9.0; 10 mM $MgSO_4$, and 10 μM $ZnSO_4$) and then centrifugation at 1,500 g for 3 min and discard the supernatant. The resulting pellets were added same amounts of zirconia beads as the pellet and 100 μl of ice-cold assay buffer with 1 mM PMSF and disrupted by vortex mixer 10 min at 4 ℃ and then 400 μl of ice-cold assay buffer with 1 mM PMSF was added. After centrifugation at 14,000 g for 1 min at 4 ℃, the resulting supernatants were processed for ALP assay. Protein contents of the resulting supernatants were determined by bradford protein assay. For ALP assay, 50μl of the resulting supernatants were added equal amounts of 2 × assay buffer with 55 mM α-naphthyl phosphate disodium salt and incubated for 20 min at 30 ℃. After incubation, the reaction solutions were added 100μl of stop buffer (2 M glycine-NaOH, pH11.0) and measured the fluorescence using wavelength of 345 nm for excitation and 472 nm for emission. The ALP activity was determined as emission per the amount of protein in the reaction (μg) and the reaction time (min).

Table I. Yeast strains used in this study.

Strains	Relevant genotype
BY4741	*MAT*a *his3Δ1 leu2Δ0 met15Δ0 ura3Δ0*
BY4741-*ole1*	BY4741 Δ*ole1*:: *CgHIS3*
SKY084	BY4741 *pho8Δ60*:: *NatMX4*
SKY100	SKY084 Δ*pep4*:: *kanMX6*
SKY084-*ole1*	SKY084 Δ*ole1*:: *CgHIS3*

Result

Yeast SCD1 homolog OLE1 is required for autophagy–To elucidate role of *OLE1* in autophagy, I constructed *ole1* mutants and confirmed that *ole1* mutants can't growth on YPD medium without supplementation oleic acid (Fig. 17A and B).

First, I investigated whether autophagic activity is increased in *ole1* mutants by starvation. In yeast, autophagy is induced nitrogen starvation (45) and can be monitored by ALP assay (43). ALP activity increased in *pho8*Δ60 cells after nitrogen starvation, but didn't increase in *pho8*Δ60 Δ*pep4* which is negative control, and *pho8*Δ60 Δ*ole1* cells (Fig. 17C). I also investigated whether inhibition of increasing of ALP activity come from cell death. As a result, cell viability was decreased in Δ*ole1* cells compare to wild-type cells, but decreasing of cell viability was milder than that of ALP activity (Fig. 17D). This result suggested that increasing of ALP activity is suppressed by depletion of UFA in ole1 mutants rather than cell death. I also indicated that ALP activity doesn't

increase in *pho8*Δ60 Δ*ole1* cells after incubation in YPD medium with 500 nM rapamycin (Fig. 17C). Tor which is yeast homolog of mTor is inhibited by rapamycin treatments, resulted in autophagy induction (22), therefore, these result suggested that Ole1 activity is required downstream of Tor in autophagy.

Next, I investigated whether cytoplasm to vacuole targeting (Cvt) pathway is suppressed in *ole1* mutants. In nutrient rich-condition, prApe1 didn't accumulate in wild-type cells, but accumulated in Δ*ole1* cells (fig. 17E). I also found that accumulation of prApe1 in Δ*ole1* cells is recovered by incubation in YPD with OA medium (fig. 17E). These result suggested that nitrogen starvation-induced autophagy and intracellular transport by Cvt pathway under nutrient rich condition are inhibited in *ole1* mutants.

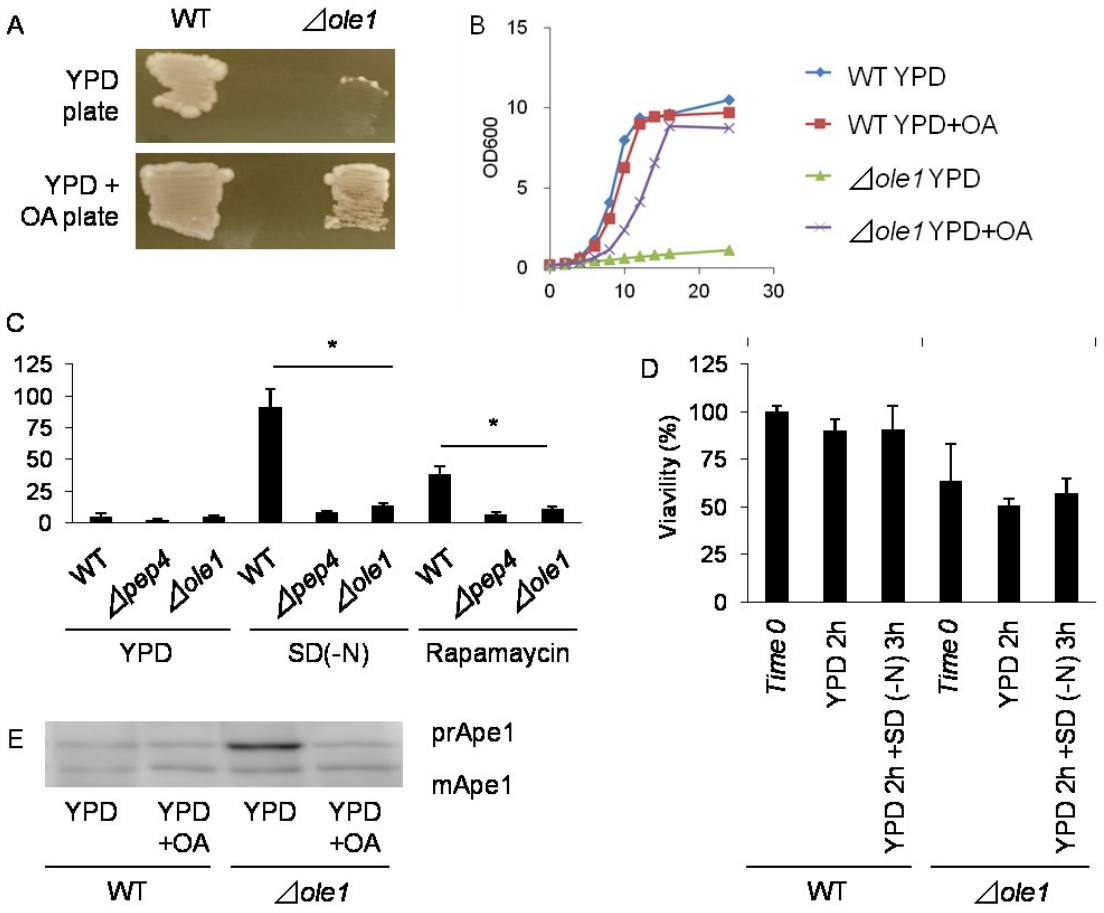

Figure 17. Yeast SCD1 homolog *OLE1* is required for autophagy. (A) wild-type (BY4741) or Δ*ole1* cells (BY4741-*ole1*) were grown on YPD or YPD with 1mM oleic acid and 1% tritonX-100 (YPD+OA) plates at 30 °C for 2 day. (B) wild-type (BY4741) or Δ*ole1* (BY4741-*ole1*) cells were grown in YPD or YPD+OA medium at 30 °C for

24h with data measurement every 2h. (C) wild-type (SKY084), Δ*pep4* (SKY100) or Δ*ole1*(SKY84-*ole1*) cells were grown in YPD, SD (-N) or YPD with 500nM Rapamycin medium for 3h after preincubation in YPD medium for 2h, and then subjected to ALP assay. ALP activity is determined as emission per the amount of protein in the reaction (μg) and the reaction time (min). Data represent means ± SE of three independent experiments. *, $p < 0.01$ (D) Viability of wild-type (BY4741) or Δ*ole1* (BY4741-*ole1*) cells was determined by counting colony number in aliquots of the culture grown on YPD or YPD + OA plates at 30°C. Data represent means ± SE of three independent experiments. (D) wild-type (BY4741) or Δ*ole1* (BY4741-*ole1*) cells were grown in YPD or YPD + OA medium for 3h after preincubation in YPD medium for 2h. The cell lysates were processed for immunoblot analysis to detect precursor Ape1 (prApe1) and mature Ape1 (mApe1).

Discussion

In this study, I investigated whether *OLE1* is required for autophagy in yeast. As a result of ALP assay, increasing of autophagic activity induced by nitrogen starvation or rapamycin treatments was inhibited in *ole1* mutants. This result suggested that Ole1 is required for nitrogen starvation induced autophagy downstream of Tor. I also performed that Cvt pathway under nutrient rich condition is inhibited by deficient of *OLE1*. Stukey et al. reported that synthesis of unsaturated fatty acid is inhibited by deficient of *OLE1*. Therefore, my results suggested that MUFA produced by *OLE1* is required for autophagy in yeast. In fact, inhibition of Cvt pathway is recovered by supplementation of oleic acid.

Given that cytochemistry has suggested that the content of unsaturated fatty acids in the isolation membrane is high (5), it is very important to determine whether MUFA produced by SCD1 or *OLE1* is used for autophagosome formation. I propose two distinct possibilities:

1. MUFA produced by SCD1 or *OLE1* can increase membrane fluidity by increasing the MUFA composition of membrane phospholipids on the ER or vacuole as pre-autophagosomalstructure . High membrane fluidity may be necessary in order to expand the isolation membranes.

2. Unsaturated fatty acids such as oleic acid are truncated cone-shaped fatty acids that can generate membrane curvature. Chan et al. reported that ULK1 recognizes and translocates to the autophagosome formation site via the C-terminal domain of ULK1 (46). Additionally, Ragusa et al. reported that the C-terminal EAT domain of Atg1 (the yeast homolog of ULK1) senses membrane curvature (47). Similar

dependency on high membrane curvature has been reported for Atg3 activity (48).

Reference

41. Miyazaki, M., Jacobson, M. J., Man, W. C., Cohen, P., Asilmaz, E., Friedman, J. M., Ntambi, J. M. (2003) Identification and characterization of murine SCD4, a novel heart-specific stearoyl-CoA desaturase isoform regulated by leptin and dietary factors. J Biol Chem. 278, 33904-33911.
42. Stukey, J. E., McDonough, V. M., Martin, C. E. (1989) Isolation and characterization of OLE1, a gene affecting fatty acid desaturation from Saccharomyces cerevisiae. J Biol Chem. 264, 16537-16544.
43. Noda, T., Klionsky, D. J. (2008) The quantitative Pho8Delta60 assay of nonspecific autophagy. Methods Enzymol. 451, 33-42
44. Scott, S. V., Baba, M., Ohsumi, Y., Klionsky, D. J. (1997) Aminopeptidase I is targeted to the vacuole by a nonclassical vesicular mechanism. J Cell Biol.138, 37-44.
45. Takeshige, K., Baba, M., Tsuboi, S., Noda, T., Ohsumi, Y. (1992) Autophagy in yeast demonstrated with proteinase-deficient mutants and conditions for its induction. J Cell Biol. 119, 301-311.
46. Chan, E. Y., Longatti, A., McKnight, N. C., Tooze, S. A. (2009) Kinase-inactivated ULK proteins inhibit autophagy via their conserved C-terminal domains using an Atg13-independent mechanism. Mol Cell Biol. 29, 157-171
47. Ragusa, M. J., Stanley, R. E., Hurley, J. H. (2012) Architecture of the Atg17 complex as a scaffold for autophagosome biogenesis. Cell. 151, 1501-1512
48. Nath, S., Dancourt, J., Shteyn, V., Puente, G., Fong, W.M., Nag, S., Bewersdorf, J., Yamamoto, A., Antonny, B., Melia, T.J. (2014) Lipidation of the LC3/GABARAP family of autophagy proteins relies on a membrane-curvature-sensing domain in Atg3. Nat Cell Biol. 16, 415-24

Conclusion

In this study, I revealed that SCD1 activity is required for the early stage of autophagy in mammalian cell. I also found that *OLE1* is required for autophagy in yeast. Therefore, I conclude that fatty acid desaturation is universally required for the autophagy in eukaryote cells.